2022-03

IMPROVING THE ENDURANCE OF SMALL UNMANNED AERIAL VEHICLES UTILIZING FLEXIBLE SOLAR CELLS

Cochella Diaz, Eduardo F.

Monterey, CA; Naval Postgraduate School

NAVAL POSTGRADUATE SCHOOL

MONTEREY, CALIFORNIA

THESIS

IMPROVING THE ENDURANCE OF SMALL UNMANNED AERIAL VEHICLES UTILIZING FLEXIBLE SOLAR CELLS

by

Eduardo F. Cochella Diaz

March 2022

Thesis Advisor: Sherif N. Michael
Second Reader: James Calusdian

THIS PAGE INTENTIONALLY LEFT BLANK

REPORT DOCUMENTATION PAGE			Form Approved OMB No. 0704-0188

1. AGENCY USE ONLY *(Leave blank)*	2. REPORT DATE March 2022	3. REPORT TYPE AND DATES COVERED Master's thesis

4. TITLE AND SUBTITLE IMPROVING THE ENDURANCE OF SMALL UNMANNED AERIAL VEHICLES UTILIZING FLEXIBLE SOLAR CELLS	5. FUNDING NUMBERS
6. AUTHOR(S) Eduardo F. Cochella Diaz	
7. PERFORMING ORGANIZATION NAME(S) AND ADDRESS(ES) Naval Postgraduate School Monterey, CA 93943-5000	8. PERFORMING ORGANIZATION REPORT NUMBER
9. SPONSORING / MONITORING AGENCY NAME(S) AND ADDRESS(ES) N/A	10. SPONSORING / MONITORING AGENCY REPORT NUMBER

11. SUPPLEMENTARY NOTES The views expressed in this thesis are those of the author and do not reflect the official policy or position of the Department of Defense or the U.S. Government.

12a. DISTRIBUTION / AVAILABILITY STATEMENT Approved for public release. Distribution is unlimited.	12b. DISTRIBUTION CODE A

13. ABSTRACT (maximum 200 words)

Though studies and experimentation have been done regarding solar UAVs, it appears that these studies have been primarily focused on the development of futuristic prototypes or proof-of-concept vehicles used under very controlled conditions and without regard to extensive practical applications. On the other hand, in this research we seek to examine the flying endurance benefits that may be achieved by equipping the Nimbus Pro VTOL small unmanned aerial aircraft with commercially available thin film photovoltaic cells.

Typical miniature and micro UAVs that run on battery power have an endurance of thirty minutes to two hours, after which time they need to be retrieved so that the batteries can be recharged, or so that another single-use battery can be installed. The retrieve-prepare-relaunch cycle can be greater than the on-station time for the UAV, and greatly reduces the utility of these systems to the intelligence gatherer or war fighter.

The focus of this research is to determine the estimation of the power consumption of the Nimbus Pro VTOL and the power generated from an array of solar cells installed on the wing of the aircraft. With that information, we can approximate the additional flight time gained by the installation of the solar array.

14. SUBJECT TERMS solar power, thin solar cell, UAV, irradiance, efficiency, power	15. NUMBER OF PAGES 113
	16. PRICE CODE

17. SECURITY CLASSIFICATION OF REPORT	18. SECURITY CLASSIFICATION OF THIS PAGE	19. SECURITY CLASSIFICATION OF ABSTRACT	20. LIMITATION OF ABSTRACT
Unclassified	Unclassified	Unclassified	UU

NSN 7540-01-280-5500 Standard Form 298 (Rev. 2-89) Prescribed by ANSI Std. 239-18

THIS PAGE INTENTIONALLY LEFT BLANK

Approved for public release. Distribution is unlimited.

IMPROVING THE ENDURANCE OF SMALL UNMANNED AERIAL VEHICLES UTILIZING FLEXIBLE SOLAR CELLS

Eduardo F. Cochella Diaz
LTJG, Peruvian Navy
Naval Maritime Science, Peruvian Naval Academy, 2014

Submitted in partial fulfillment of the
requirements for the degree of

MASTER OF SCIENCE IN ELECTRICAL ENGINEERING

from the

NAVAL POSTGRADUATE SCHOOL
March 2022

Approved by: Sherif N. Michael
Advisor

James Calusdian
Second Reader

Douglas J. Fouts
Chair, Department of Electrical and Computer Engineering

THIS PAGE INTENTIONALLY LEFT BLANK

ABSTRACT

Though studies and experimentation have been done regarding solar UAVs, it appears that these studies have been primarily focused on the development of futuristic prototypes or proof-of-concept vehicles used under very controlled conditions and without regard to extensive practical applications. On the other hand, in this research we seek to examine the flying endurance benefits that may be achieved by equipping the Nimbus Pro VTOL small unmanned aerial aircraft with commercially available thin film photovoltaic cells.

Typical miniature and micro UAVs that run on battery power have an endurance of thirty minutes to two hours, after which time they need to be retrieved so that the batteries can be recharged, or so that another single-use battery can be installed. The retrieve-prepare-relaunch cycle can be greater than the on-station time for the UAV, and greatly reduces the utility of these systems to the intelligence gatherer or war fighter.

The focus of this research is to determine the estimation of the power consumption of the Nimbus Pro VTOL and the power generated from an array of solar cells installed on the wing of the aircraft. With that information, we can approximate the additional flight time gained by the installation of the solar array.

THIS PAGE INTENTIONALLY LEFT BLANK

TABLE OF CONTENTS

THIS PAGE INTENTIONALLY LEFT BLANK

LIST OF FIGURES

THIS PAGE INTENTIONALLY LEFT BLANK

LIST OF TABLES

THIS PAGE INTENTIONALLY LEFT BLANK

LIST OF ACRONYMS AND ABBREVIATIONS

A	amps
CIGS	copper-indium-gallium selenide
DC	direct current
EEMS	electrical energy management system
EM	electromagnetic
RFID	radio frequency identification
MPPT	maximum power point tracker
PV	photovoltaic
SUAV	small unmanned aerial vehicles
TFPV	thin-film photovoltaic
UAV	unmanned aerial vehicle
VTOL	vertical take-off and landing
W	watts

THIS PAGE INTENTIONALLY LEFT BLANK

EXECUTIVE SUMMARY

Unmanned aerial vehicles (UAVs) are aircraft that are piloted autonomously and/or remotely and are equipped with sensors, target designators, offensive munitions, or electronic transmitters with the purpose of interfering with or destroying enemy targets. They have been in use by United States military forces in the decades following WWII. According to [1], in addition to reconnaissance and combat roles, the armed forces have also been focusing on "expeditionary energy" in order to reduce logistical requirements [1].

Solar power has become a feasible choice for powering unmanned aircraft (UAV, UAS, RPAS, drones) because of recent advances in photovoltaic (PV) technology. Efficiency is the most frequently used metric for measuring the performance of solar technology. This metric, which is impacted by wavelength, reflectance, and temperature, is a metric that indicates how much of the energy from the sun can be converted to useable electrical energy [2].

Modern small unmanned aerial vehicles (SUAV) have a flying duration of about 90 minutes due to battery life limitations, and the push toward alternative energy sources necessitates that such systems be efficient. As a result, increasing the capacity and durability of current UAVs becomes a priority in order to improve the warfighter's fighting effectiveness while also lowering Department of Defense operations expenses [3].

Solar efficiency rates for single-junction solar cells now stand at 29.1% and for multi-junction solar cells at 31.6%. Multi-junction PVs employ many layers to collect light at various wavelengths, enabling them to achieve better efficiency than single-junction solar cells. The disadvantage is that the production process is more difficult and costly, which makes PVs more ideal for high-end solar UAV initiatives.

Additionally, the power-to-area ratio is important to take into account. Even on large fixed-wing solar UAVs, the available surface for solar cells is constrained. Increases in the wingspan of an unmanned aircraft to permit useful element solar cells may lead to an increase in weight and drag that is not offset by the increase in solar power.

References

[1] J. Guilmartin, “Unmanned aerial vehicle,” Encyclopedia Britannica, blog, 2020. https://www.britannica.com/technology/unmanned-aerial-vehicle

[2] L. Mansfield, “Copper Indium Gallium diselenide solar cells,” Photovoltaic Research, blog. https://www.nrel.gov/pv/copper-indium-gallium-diselenide-solar-cells.html (accessed Oct. 24, 2021).

[3] AeroVironment, Inc, “Puma™ 3 AE,” AV AeroVironment, blog, 2021. https://www.avinc.com/uas/puma-ae

ACKNOWLEDGMENTS

I would like to thank God first for helping and guiding me during this rich time of my life, lived at the Naval Postgraduate School.

I would like to thank the Peruvian Navy for giving me the opportunity to come to study for this amazing master's degree at this prestigious institution.

I would like to thank my parents, who have stayed with me in each step of my life, teaching me and being my guide. I am grateful for the education and values that they gave me during my childhood that nowadays help me to be a good Naval Officer and Citizen.

I would like to express my gratitude to Professors Sherif Michael and James Calusdian for directing my study and offering sound advice during this process.

I would like to thank the friends that I made during these two years and three months of intensive studies at the Naval Postgraduate School for helping me every time I needed it.

Finally, I would like to thank a very special person, a person whom I consider like a brother, friend, and partner. A friend who has just passed away, after a long battle against cancer. Thank you, Mauricio Angulo, for your friendship, for teaching me that it does not matter how difficult life can be—there is always a reason to smile. Thank you, because you taught me to be the bravest person. Thank you for all these years of long conversations and smiles. Thank you for being my friend.

THIS PAGE INTENTIONALLY LEFT BLANK

I. INTRODUCTION

A. BACKGROUND

Unmanned planes, also known as unmanned aerial vehicles (UAVs) or drones, date back to before the First World War and have been employed in some capacity in nearly every conflict since the Second World War by almost every foreign military [1]. In the early 1980s, the Israeli Security Forces outfitted unmanned aircraft that resembled large model aircraft with trainable television and thermal imaging cameras as well as beam missile objective identifiers that were all transmitted to a command center. These vehicles were excellent in battlefield observation and target identification because of their tiny size and silent engines, which made them nearly undetectable [2].

UAVs today perform a wide range of tasks, including weather surveillance, search and rescue operations during natural catastrophes, photography, videography, and cargo delivery. The military, however, uses them for reconnaissance, surveillance, and targeted assaults, which is the most well-known and contentious application. Since the terrorist events of September 11, 2001, the United States has dramatically boosted its use of drones. They are mostly employed for observation in places and terrains where personnel cannot safely operate [3]. UAVs are, of course, becoming a more vital element of the military in many nations. The U.S. armed services now operate a fleet of tens of thousands of UAVs. Nevertheless, the quantity of UAVs in private use dwarfs this. According to the Federal Aviation Administration (FAA), 1.1 million UAVs were registered in the U.S. in 2019 [4].

A fixed-wing UAV is one form of UAV that may be used to carry out a flying task. Because the battery used in this type of drone has a limited capacity, especially in micro-scale UAVs, the flight time is limited. As a result, the drone may need to return before the mission is completed to replace the batteries. Experimental studies that include solar cells in the UAV wing design to enhance flying duration are warranted. Designing electronic components for UAVs that are compatible with solar cell charging systems is a primary goal in this area of research [5].

When considering that a significant percentage of battery energy is expended on takeoff, navigation into and out of the monitored area, and landing/recovery, there is relatively short time left to accomplish the in-flight mission. Solar cells provide a possible solution [6].

The high correlation between Figures 1 and 2 demonstrates how many countries deploy armed drones in areas with a lot of sunshine. This correlation can be beneficial in determining the potential advantages for such countries. Thin-film photovoltaic (TFPV) cells were developed to lower the weight required to generate power while simultaneously providing flexibility and durability. The efficiency of solar cells has steadily improved over time as a result of greater research and development, allowing them to produce more electricity on the same available surface area as other forms of technology.

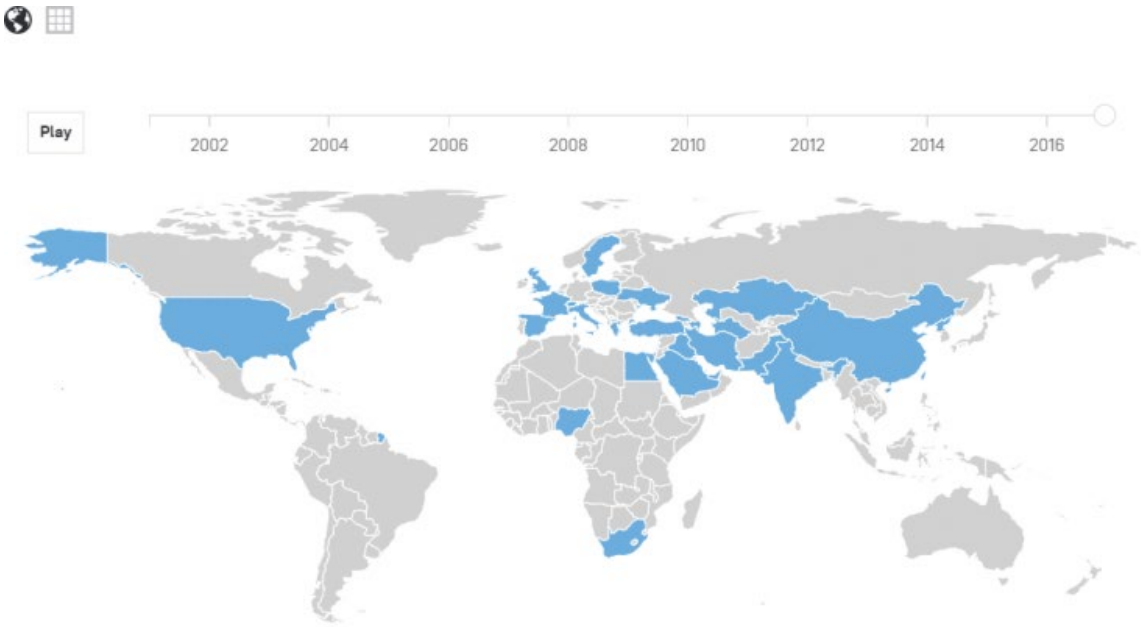

Figure 1. Armed drone-wielding countries. Source: [4].

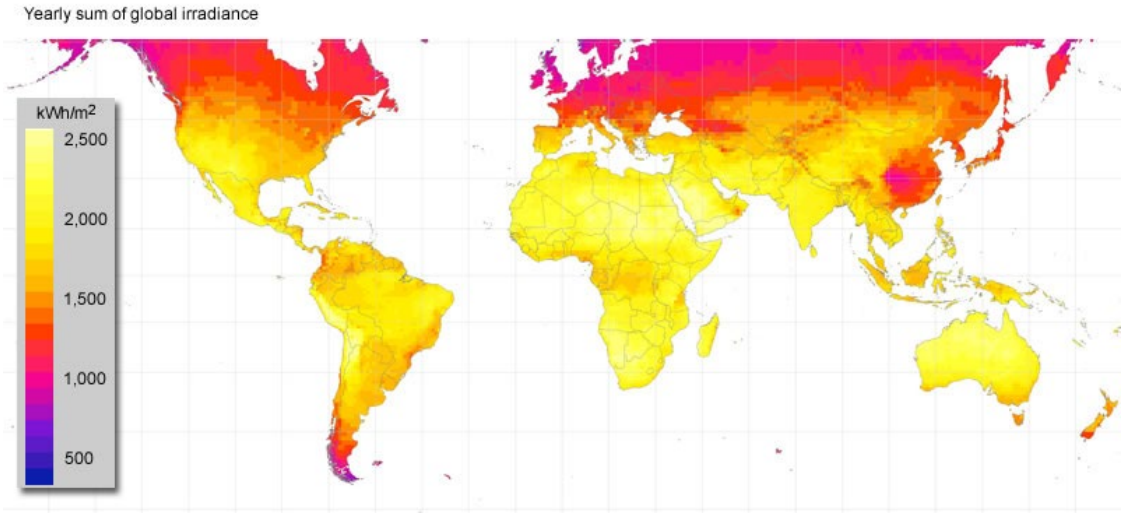

Figure 2. Solar irradiation on an annual basis. Source: [6].

B. OBJECTIVE

This objective of this thesis is to employ commercially available components to improve the endurance of a current SUAV with modest modifications. The additional power will be obtained by attaching CIGS cells to a SUAV wing without considerably raising aerodynamic drag or electrical load, thanks to their flexible and lightweight properties.

The viability of this approach will be determined by comparing the weight and cost of modifications against the increased flying duration. As the performance of these cells improves, they may eventually be able to transition from delaying battery depletion to full in-flight recharging. UAV flight time would be considerably increased if batteries could replenish while still in the air. Under this scenario, systems will be allowed to self-charge energy storage devices and possibly other systems while on the ground between flights. Solar energy would reduce UAV dependency on automobiles and other external power sources, as well as the need for extra batteries.

This technique could be applied to tactical and analytical UAVs, as well as enforcement agencies and commercial products.

C. RELATED WORK

This research continues previous Naval Postgraduate School research on the use of solar energy to power SUAVs. In 2009, William R. Hurd worked with a recreational aircraft designed to resemble an armored truck and discovered that by adding solar cells, flight endurance could be about tripled [7]. Javier V. Coba purchased a Raven UAV in 2010 and estimated that a modified wing would increase performance by 33–100%, depending on the amount of throttle used [8]. The apparatus was unable to fly due to the lack of an adequate airfoil on the wing. Chee Keen Chin built a computational model based on the findings of Coba's thesis in order to design his own solar cells in 2011 [9]. By mounting the photovoltaic (PV) cells on an airplane wing that strongly resembles that of a Raven, testing according to appropriate procedures, collecting data at each power setting, and accounting for solar movement during lengthy daytime testing, this research offered many lessons in design optimization. Finally, in 2012, Christopher R. Gromadski demonstrated the feasibility of boosting an onboard power source using enhanced TFPV cells consisting of copper-indium-gallium selenide (CIGS) cells over a greater duration of time (CIGS) [6].

D. APPROACH

The initial stage in this research was to simulate a model with the same wingspan as a Nimbus PRO vertical take-off and landing (VTOL) so that it could be validated and tested using a real-world system. To show the proportional improvement and the test limit variables, the Nimbus PRO VTOL current demands and battery endurance were analyzed.

Using a comparable Nimbus PRO VTOL wing and airfoil as a template, we created a redesigned wing to suit the projected solar array while ensuring optimum lift to counteract increases in drag and weight owing to increased circuitry. Then, we acquired the most efficient thin flexible cells that were obtainable; in this case, we utilized CIGS cells because they are the most efficient solar cells accessible in terms of cost and weight. The cells were evaluated before and after encapsulation to ensure they were efficient and that the mounting was effective. Following installation, the circuitry, which included a maximum power point

tracker (MPPT) and a direct current (DC)-to-DC power converter, was linked and tested to ensure that it worked properly and that the power system was as efficient as possible.

The simulation of the Nimbus PRO VTOL was evaluated in a bench-mounted setting for current demand and battery longevity, either with or without solar array input. Throughout the testing, the percentage of current input to the system was displayed to demonstrate the observed variance in sunshine over the course of a day. To assess system potential, the findings were updated to account for individual and cumulative changes in circuitry.

E. ORGANIZATION

The different varieties of SUAVs available in both the military and civilian markets are examined in Chapter II, along with their features, performance, specifications, and advantages and disadvantages.

Lithium-ion batteries are explored in Chapter III because they are among the highest power ratios, a high ideal voltage source, a reduced self-rate, no storage impact, and a slow loss of charge while not in use. Additionally, lithium-ion batteries are rapidly being embraced in military, electric car, and aerospace industries because of their high energy density.

Chapter IV will discuss the theory of solar cell operation, as well as variables affecting their performance, and even the types and fabrication of flexible solar cells. The advantages and disadvantages of each will be highlighted, including why CIGS cells are the best solution. Also, DC-to-DC converters are analyzed in Chapter IV.

Chapter V is a continuation and enhancement of Chapter IV since it describes the properties and advantages of CIGS solar cells in great detail.

The relevance and purpose of the connections between the solar panel and the battery to maintain the quantity of power are discussed in Chapter VI. The functioning of MPPTs, electrical energy management systems (EEMS), and battery balancers is also covered in this chapter.

In Chapter VII, we have estimated the power consumption of the Nimbus Pro VTOL, approximating that number based on the information available on this aircraft. We then estimated the power generated from an array of solar cells installed on the wing of the aircraft. Finally, with estimates of power consumption for the UAV and the power generated by the solar cells, we proceeded to approximate the additional flight time gained by the installation of the solar array.

Chapter VIII is a summary of what we have achieved during the process.

II. SMALL UNMANNED AERIAL VEHICLES

A. SELECTION CRITERIA

The prevalence of SUAVs is increasing rapidly in both military and civilian applications. One important characteristic of SUAVs is the flying time they can achieve, which is limited by the energy storage available onboard the aircraft. The main benefit solar cells attached to the surface of the wings can provide is a boost to the energy available for the SUAV. The characteristics of the different types of SUAV are extremely important when it comes to selecting which type of solar cell would be the best choice. This investigation hopes to enhance airframe endurance through the use of PV panels, with the main goal of charging rechargeable battery packs mid-flight.

To accomplish these goals, numerous criteria must be examined, including the following:

- The wing surface area on the SUAV where solar cells can be deployed. This aspect can be very critical because the total input power to the whole system can be directly proportional to the area of the wings.

- Since the objective of the solar cell is to obtain energy from the sun and replenish the battery during the flight to extend endurance, the battery power source must be rechargeable. We seek to optimize the charge delivered to the battery from the solar cells without sacrificing the flight performance of the SUAV airframe.

- The SUAV must have payload capabilities that help to achieve the ultimate goal of the users. In military applications, payloads range from relatively light surveillance sensor packages to weapons that may weigh more than the airframe itself.

In that sense, the following systems meet the criteria of being part of the possible options to analyze considering the pros and cons including the above selection criteria.

B. TACTICAL DRONES - RAVEN RQ-11A/B

AeroVironment is the company in charge of the development of the RAVEN RQ-11A/B that was first placed in service in 2003. This type of UAS was developed for quick response and high flexibility in support of military and civilian missions needing monitoring and intelligence gathering [10], which is widely regarded as its most productive mission with the U.S. armed forces. The RAVEN RQ-11A/B possesses the ability to act manually or autonomously [6].

According to the specifications, the RAVEN RQ-11A/B has a wingspan of 4.5 ft (1.4 m), an endurance of 60–90 min, and a maximum speed of 81 km/h (44 knots). Having a weight of 4.2 lbs. (1.9 kg), the aircraft is launched by hand [10].

There are some disadvantages that must be considered and those are the limited capabilities of the dual forward and side-look EO nose camera, electronic pan-tilt-zoom with stabilization, and forward and side-look IR nose camera (6.5 oz payloads) [10]. The Raven RQ-11A/B is shown in Figure 3.

Figure 3. Launching the RAVEN RQ-11A/B

C. FIXED-WING DRONES

The secret to the success of the fixed-wing aircraft was its design. While a multirotor constantly draws a lot of battery power to spin its propellers enough to generate

lift, a fixed wing only needs the power for propulsion**.** The lift of the aircraft is generated passively by its wings that cut the air at a certain angle. That means these systems can fly much longer and cover much more ground than multiple rotors [11].

Some fixed-wing drones are fueled by gas. A fixed-wing drone can stay in the air for up to 16 hours of continuous flight, whereas multi-rotor units can only stay in the air for a few minutes. Fixed-wing drones cannot, however, hover in the same manner as drones with helicopter-style rotors [1].

Also, there are some disadvantages that have to be considered. These systems, for starters, necessitate big, open, and relatively soft landing surfaces. If a football or soccer field is nearby, the risk is reduced. If not, searching for similar sites on a mine field, building site, or forested site can be time-consuming and dangerous. When low-altitude winds blow or planning errors surface that cannot be corrected once landing has commenced, belly-landing UAVs have been known to crash into trees or obstructions if the landing area is not large enough. Also, when the fixed-wing lands in a wide-open region, it undergoes a controlled crash, every single time. The drone and payload life spans are shortened as a result of the shock. Finally, the traditional, hand-launched, belly-landing fixed-wing drones must be lightweight because they must be thrown into the air and land as described. This means that the payload will always have a weight limit, which is a problem because higher-end payloads are heavier [11]. A fixed-wing drone is shown in Figure 4.

Figure 4. Launching a fixed-wing drone

D. PUMA 3 AE

The AeroVironment-developed PUMA 3 AE (All Environment) comes with a large Mantis i45 EO/IR payload and is capable of performing missions during day, nighttime, or limited settings, as well as on land or sea. It has a strengthened fuselage with an alternative under-wing transition room for supplemental payloads and third-party programs, as well as a variety of different programs (M1/2/5 and M3/4/6), all of which are protected by strong AES 256-bit encryption. The enhanced launch vehicle on the Puma 3 AE makes manual or automated launch substantially more accessible and reliable [12]. Additionally, it has a range of up to 15 kilometers and the ability to remain in stationary orbit for more than 120 minutes. In addition to the power consumption of the motor, the range and loiter time are determined by a variety of additional factors such as battery characteristics, avionics, and servo actuators. The Puma AE is launched manually, follows a pre-programmed GPS path, flies as high as 45 mph at 500 feet AGL, and lands on large areas of ground utilizing a standard bottom descent. The Puma AE is fitted with a gyrostabilized payload that works at an angle of plus or minus 180 degrees and leans at an angle of plus 10 to minus 90 degrees. Additionally, it features an EO and an infrared sensor as well as infrared lighting.

The Puma AE communicates on UHF L-band frequencies through the AeroVironment JCIGCS to offer FMV, take photos, and preserve data for replay during target evaluation [13].

The system still has certain faults, however. Individual components of the system weigh much more than those on a Raven, limiting the PUMA 3 AE mobility. As with the Raven, the system is designed for a high-pitch descent, which may have an effect on durability and any PV cells placed on the airfoil. Figure 5 shows the launch of a PUMA 3 AE.

Figure 5. Launching the PUMA 3 AE

E. MILVUS VTOL

MILVUS, detailed in Table 1 and shown in Figure 6 [14], uses a revolutionary fixed-wing system with the VTOL function that allows for unlimited take-off and landing by mitigating the challenges of typical fixed-wing systems [14].

In a short amount of time, it may survey open regions such as rivers and prairies, as well as monitoring the vegetation index of national parks and grasslands. It may be used

for surveillance and reconnaissance across large regions, such as international boundaries, at any time of day or night [14].

Table 1. MILVUS VTOL specifications. Source: [14].

Operating Speed	58–80 km/h (16–22 m/s)
Operating Time	60~80 min
Maximum Flying Speed	120 km/h (33 m/s)
Payload	24 MP Sony A6000, E0/IR, Multi-Spectral Sensor
Loading Capacity	700 g
Unit Weight	4.1 kg
Maximum Take-off Weight	7 kg
Size	2000*770*300
Purposes	Survey, Patrol/Monitoring

Figure 6. Milvus VTOL. Source: [14].

F. NIMBUS VTOL

The NIMBUS VTOL, detailed in Table 2 and shown in Figure 7, demonstrates how technological advancements have opened the path for a range of unmanned aircraft implementations. VTOL small unmanned aircraft systems comprise rotary- and fixed-wing aircraft, as well as hybrid systems that combine rotary and fixed-wing capabilities. These aircraft are said to possess a variety of benefits. These aircraft can also be used in agriculture for aerial mapping and digital imagery. Additionally, they may be utilized in the development of buildings and structures, as well as travel to dangerous or harmful locations for humans [3].

VTOL aircraft have several major advantages, including a smaller launch and recovering zone, rapid deployment, and translational capabilities. Each of these characteristics contributes to aircraft suitability for a range of applications, including precision agriculture, emergency response, and military transportation. For farmers, for example, the ability to deploy an aircraft horizontally without having a path is particularly tempting. It enables them to get aerial photographs without deploying a manned aircraft, which frequently requires the use of a runway [3].

Foxtech in China is a leading reseller of commercial products within this industry; such industrial aircraft may be used for a range of business purposes, including monitoring, imaging, and power line inspection. NIMBUS VTOL Mapping Version is one of their newest offerings for remote sensing applications [15].

The NIMBUS VTOL is a three-rotor VTOL with vector yaw that features power reliability and is capable of lifting up to 500g (almost a pound). With one 6S 10000mAh Lipo battery, the highest maneuvering speed is 35 m/s, and the flight time is around one hour, including take-off and landing. In the event of a system malfunction, the Nimbus VTOL may automatically switch to a multirotor configuration and reach the ground safely. The drone can take off from an area as small as 3x3 meters. The flight endurance of the NIMBUS VTOL is up to 60 minutes [15].

Table 2. NIMBUS VTOL specifications. Source: [16].

Version	Nimbus VTOL
Wingspan	1800 mm
Length	1300 mm
Suggested Take-off Weight	6 km
Suggested payload	800 g
Total Weight	3.36 kg (no battery)
Max. Flying Height	3500 m
Max. Flying Speed	35 m/s
Average Speed	15 m/s to 16 m/s
Stall Speed	10 m/s to 11 m/s
Max Wind Resistance	<10.7 m/s
Mapping Accuracy	Centimeter
Suggested Battery	6S 12000 mAh Lip Battery

Figure 7. NIMBUS VTOL

G. NIMBUS PRO VTOL

Nimbus Pro is a fixed-wing VTOL aircraft, detailed in Table 3 and illustrated in Figure 8, for surveying, aerial mapping, and surveillance missions. Dimensions are shown in Figures 9, 10, and 11. The mapping VTOL is propelled upward by four lift propellers and one fixed-wing engine, similar to a helicopter. For mapping purposes, the fixed-wing motor will propel the drone like an airplane [17]. The Support 6S battery is shown in Figure 12.

Shenzhen Yangda Security Co. is a renowned online vendor of fixed-wing planes and VTOL vehicles in China. These commercial drones are capable of measuring, tracking, inspecting electrical lines, and performing a variety of other corporate functions [17].

Table 3. NIMBUS Pro VTOL specifications. Source: [17].

MTOW	8.6 kg
Weight without battery and payload	4.03 kg
Wingspan	1950 mm
Length	1300 mm
Battery weight (Tattu 6s 25000mAh)	2.56 kg
Max payload (battery included)	4.57 kg
Suggested payload weight	1.5 kg
Endurance (no payload)	100 minutes
Cruise speed	72 km/h
Max speed	90 km/h
Stall speed	39.6 km/h
Anti-wind capability	38 km/h
Operating Altitude (Max.)	3500 m
Material	EPO, Aluminum-plastic Film, PVC
Take-off/Landing	VTOL
Working Voltage	6S
Package size	135x41x40 cm

Figure 8. Nimbus Pro VTOL. Source: [17].

Figure 9. Nimbus Pro VTOL rotors and propellers. Source: [17].

Figure 10. Nimbus Pro VTOL dimensions. Source: [17].

Figure 11. Nimbus Pro VTOL box dimensions. Source: [17].

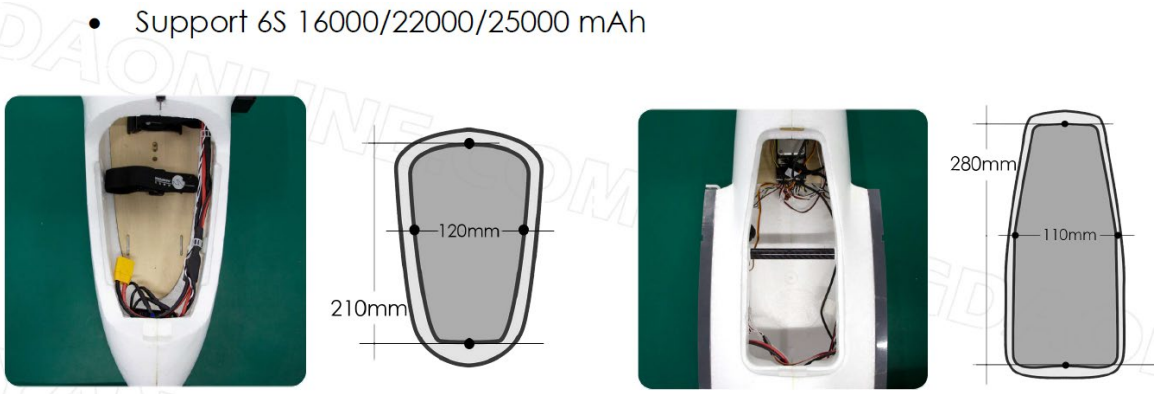

Figure 12. Battery dimensions. Source: [17].

H. CONCLUSION

The UAVs introduced here have large wingspans of between 4.5 and 9 feet and varied ranges of endurance. On the basis of take-off and landing qualities, as well as a mix of a large wingspan, a long initial lifespan, and sophisticated payloads, the NIMBUS PRO VTOL is the most capable option for PV enhancement. Contributing to the enhancement of endurance characteristics during flight, this design would need to maximize the capacity

to handle accessible sunlight while adhering to a certain robustness, frequency control, and security criteria for military applications. As the principles and limitations of photovoltaics are explained in the next chapter, the critical nature of available PV contact area and the eligibility criteria becomes increasingly apparent [6].

THIS PAGE INTENTIONALLY LEFT BLANK

III. LITHIUM-ION BATTERIES FOR SUAV

A. INTRODUCTION

Inside a lithium-ion battery, lithium ions flow from the negative terminal to the positive terminal during discharge and back to the negatively charged electrode during charging. The composition, capacity, pricing, and security characteristics of various lithium-ion battery types differ. With the exception of lithium primary batteries (which are not rechargeable), lithium-ion batteries employ an interlayer lithium mixture as the electrocatalyst instead of metallic lithium [18].

In consumer electronics, lithium-ion batteries are often used. They have one of the highest power-to-weight ratios, a high ideal voltage source, low self-rate, no memory effect, and a moderate rate of charge loss when not in use, making them one of the most popular rechargeable battery types for portable gadgets. Due to their high energy density, lithium-ion batteries are gaining traction in the military, electric vehicle, and aerospace industries [18].

1. History of Lithium-Ion Batteries

In the 1970s, M. S. Whittingham of Binghamton University proposed lithium-ion batteries. Whittingham used titanium (II) sulfide for his cathode and lithium metal for his anode. Rachid Yazami et al. established the reversible intercalation of lithium into graphite in a lithium/polymer electrolyte/graphite half-cell for the first time in 1980. In 1981, Bell Labs developed a viable graphite anode as a lithium metal battery alternative. Since Sony Corporation introducted lithium-ion batteries in 1991, they have been widely recognized as a power source for a variety of applications, including portable gadgets and electric/hybrid electric vehicles. Despite their commercial success in a number of applications, LIBs have not been deployed in large-scale electrical energy storage applications because of escalating costs and a limited supply of lithium, as seen in Figure 13 [18].

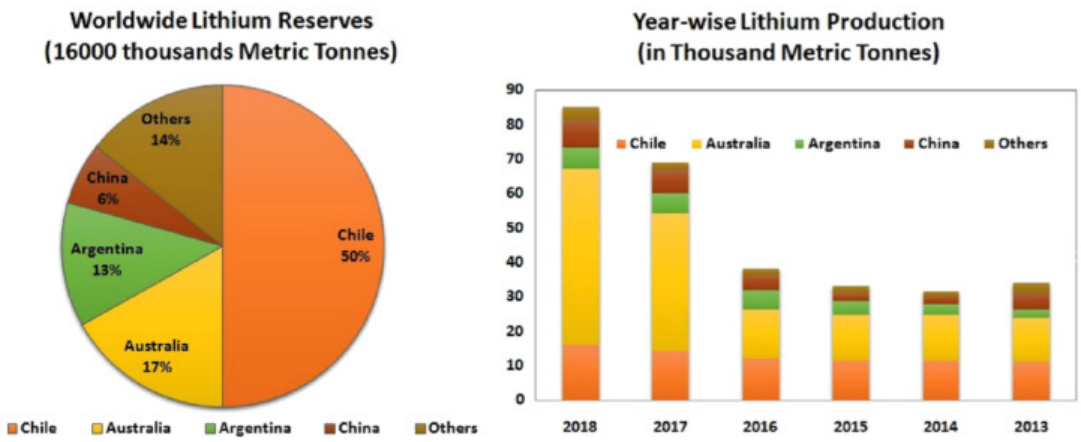

Figure 13. Reserves and production of lithium metal from 2013 to 2018. Source: [19].

2. How Lithium-Ion Batteries Work

Millions of people rely on lithium-ion batteries to power their devices every day. Due to its low weight, high efficiency, and rechargeability, this technology is becoming more used in a variety of applications, ranging from computers and smartphones to hybrid electric vehicles [20].

An anode, a cathode, a separator, an electrolyte, and two principal collectors comprise a battery (positive and negative). The lithium is contained in the anode and cathode. The electrolyte transports lithium batteries with positive electrodes from anode to cathode and vice versa via the separator. The movement of lithium ions in the anode leads to the creation of free electrons, which creates a charge at the positive current collector. After passing via a powered device, the electrical current flows from the conductive substrate to the negative collector (cell phone, computer, etc.). The separator obstructs the free passage of electrons within the battery [20], shown in Figure 14.

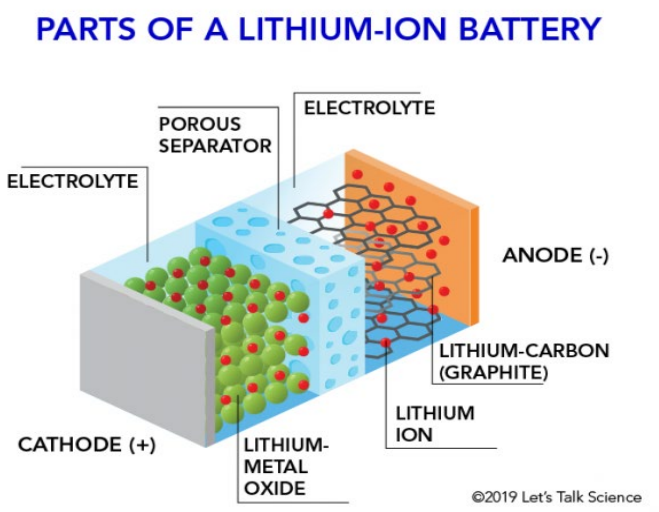

Figure 14. Parts of a lithium-ion battery. Source: [18].

When a phone is powered by a lithium-ion battery, charged particles called lithium ions (Li+) flow from the negative anode, through the electrolyte, to the positive cathode. In contrast, as seen in Figure 15, electrons circulate from the anode, through the connected external load, to reach the cathode [18].

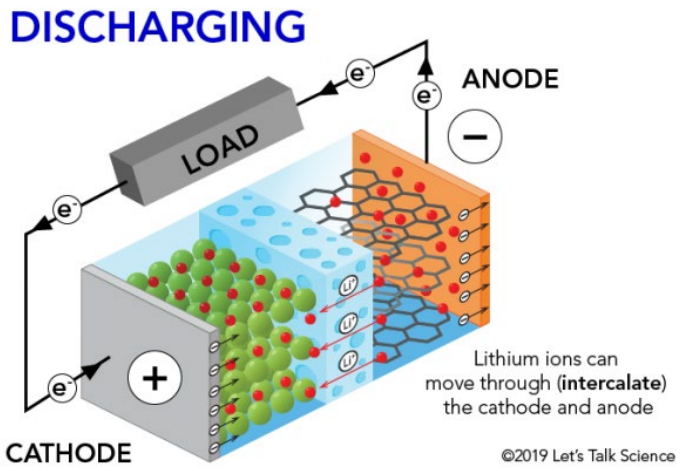

Figure 15. Discharging process. Source: [18].

The technique is exactly the reverse when a lithium-ion battery is charged. The lithium ions at the cathode travel back through the electrolyte to the anode. Electrons are transferred from the anode to the cathode because of the externally applied charging voltage. The charge/discharge cycle can be repeated hundreds of times [18].

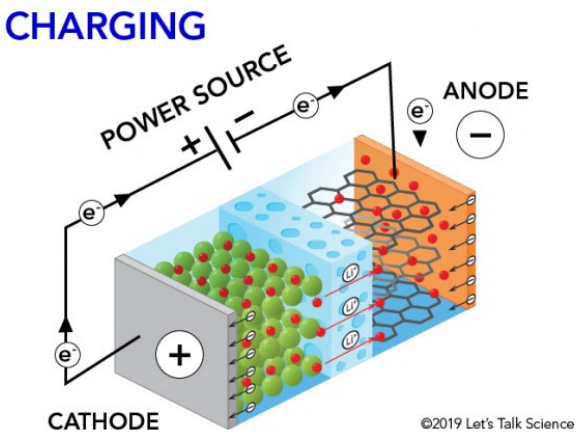

Figure 16. Charging process. Source: [18].

B. CHEMISTRY INVOLVED IN LITHIUM-ION BATTERIES

Lithium batteries have a positive electrode (cathode) made of lithium cobalt oxide and a negative electrode (anode) made of high-crystalline unique carbon. Also available is an organic solvent designed for use with certain carbon processes, such as electrolytic fluid. During charge and discharge operations, the chemical process inside the battery is shown in Figure 17.

$$LiCoO_2 + C_6 \underset{\text{discharge}}{\overset{\text{charge}}{\rightleftharpoons}} Li_{1-x}CoO_2 + C_6L_x$$

Figure 17. Chemical process. Source: [21].

The chemical reaction is based on the fact that lithium in the positive electrode material is ionized during charging and then flows from layer to layer in the negative electrode. Li ions travel to the positive electrode upon discharge, where they encapsulate the original molecule [21].

1. Features of Lithium-Ion Batteries [21]

- High energy density (volumetric energy density) of 400 Wh/L or 160 Wh/Kg (mass energy density).
- High cell voltage, compared to other types of batteries. Newer Li-Ion batteries have a nominal voltage of 3.6V or even 3.7V.
- There is no memory effect. They can be charged at any time, although they are not as long-lasting as NiMH or NiCd batteries.
- Typical operating voltage ranges from 2.8 to 4.2 volts.

Typical charging characteristics are shown in Figure 18.

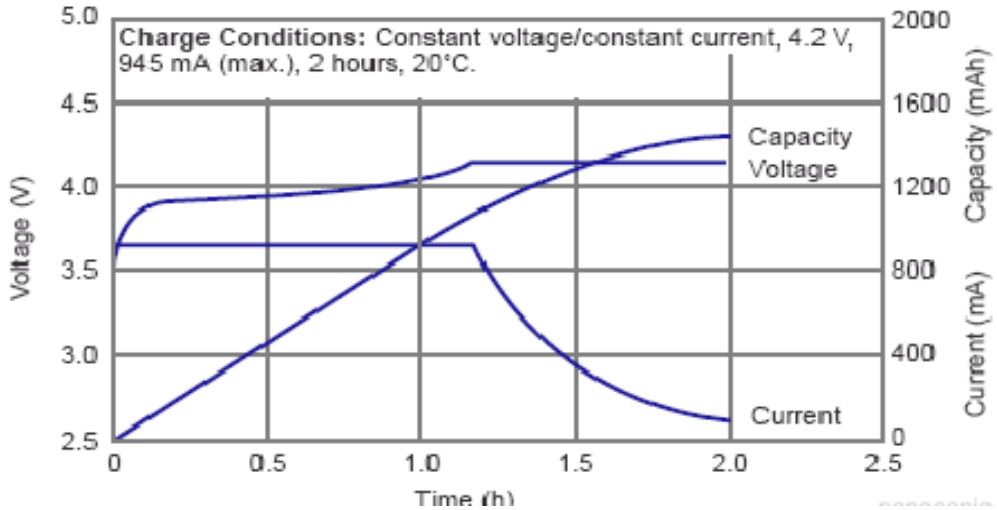

Figure 18. Typical capacity characteristics over charge cycles. Source: [21].

2. Advantages

Using a lithium-ion battery has significant advantages in many applications, from small electronic devices to cellphones and laptops, as well as autos and a range of other applications [22].

Due to the benefits of Li-ion innovation, these cells are increasingly used in a number of applications, [22].

The following are some of the advantages of lithium-ion batteries:

- High power density: One of the lithium-ion battery technology significant benefits is its high energy density. There will always be a demand for batteries with a higher energy density, as electronic devices such as smartphones must function for longer periods of time among charges while using more power. Additionally, there are several power applications, ranging from hand tools to electric autos. Lithium-ion batteries significantly outperform other types of batteries in terms of power efficiency. Additionally, electric cars require battery technology with a high energy density [22].

- Self-discharge: The rate at which many portable batteries self-discharge is a concern. Lithium-ion cells self-discharge at a much slower rate than some other reusable cells such as Ni-Cad and NiMH. It is often greater than 5% for the very first 4 hours after charging, but then reduces to roughly 1% or 2% every month [22].

- Low maintenance: A time-saving advantage of lithium-ion batteries is that they do not need to be maintained to keep working [22]. Unlike Ni-Cad cells which must be regularly discharged to prevent the memory effect or lead-acid cells need regular refilling, lithium-ion batteries require no regular maintenance [22].

- Cell Voltage: Each lithium-ion cell generates around 3.6 volts. This has a plethora of advantages. Each lithium-ion cell has a greater voltage than conventional nickel cadmium, nickel metal hydride, and even ordinary

alkaline batteries, at around 1.5 volts for alkaline and nearly 2 volts per cell for lead acid, which means that many battery applications require less cells. For smartphones, an individual cell suffices, which simplifies power efficiency [2].

3. Disadvantages

While lithium-ion batteries offer tremendous technical promise, they have a number of disadvantages, most notably in terms of reliability. Lithium-ion batteries are prone to overheating and degradation at high voltages. In rare cases, this might result in heat dissipation and ignition. This has led to significant problems, including the grounding of Boeing 787 airplanes in response to allegations of onboard battery fires. Numerous shipping firms have refused to carry batteries in bulk via plane owing to the inherent dangers of these batteries. Lithium-ion battery safety measures are necessary to manage voltage and compressive stress, which might result in weight and performance increases in specific cases [23].

Lithium-ion batteries are also prone to aging, which results in power dissipation and frequent failure over time. Their cost, which is approximately 40% more than that of Ni-Cad, is another factor preventing broad implementation. Identifying and resolving these issues is a critical component of modern technological research. Finally, while Lithium-ion batteries have a better energy density than earlier generations of batteries, they still are roughly 100 times less power dense than fuel (12,700 Wh/kg mass or 8760 Wh/L volume) [23].

THIS PAGE INTENTIONALLY LEFT BLANK

IV. SOLAR CELLS

A. INTRODUCTION

A solar cell, sometimes referred to as a PV module, is a device that directly converts light energy to electrical energy via the PV effect. A large percentage of PV cells are built of silicon, which has increased in performance and effectiveness as the technology has advanced from amorphous (non-crystalline) silicon through polycrystalline silicon to crystalline (crystalline phase) silicon. With exception of batteries or fuel cells, solar cells create energy without chemical processes or the need for fuel, and unlike electric generators, they have no moving parts [24].

Several variables affect the performance of solar cells, however. To begin, a solar cell must be exposed to a significant amount of sunlight. The cells must be constructed of materials capable of efficiently absorbing and converting the photon energy into electrical current flow. Finally, the cells must be protected from factors that might impair their function. These factors are thoroughly examined in this research, and analyses across current cell technologies are made to select the most appropriate type of cell for this investigation [6].

B. CHARACTERISTICS OF SUNLIGHT

In space, the solar spectrum includes a wide range of wavelengths. The Earth surface, on the other hand, absorbs the selected sunlight, which is restricted by the atmosphere to a specific range of wavelengths. Sunlight is made up of photons, tiny particles that transport electromagnetic (EM) waves from the sun as they move through space. Except for those with lower energy levels, all photons that reach a solar cell can be turned into electricity. Those with greater energy levels must use the thermalization of photo-generated carriers to reduce their energy content to the gap energy for successful energy conversion. Figure 19 shows the solar radiation spectrum on Earth; the extraterrestrial radiation distribution is described by the solar spectral irradiance curve, which spans a wide range of wavelengths. The atmosphere, on the other hand, attenuates

many portions of the spectrum and significantly affects the solar energy delivered to the Earth surface by, for example, removing X-rays [25].

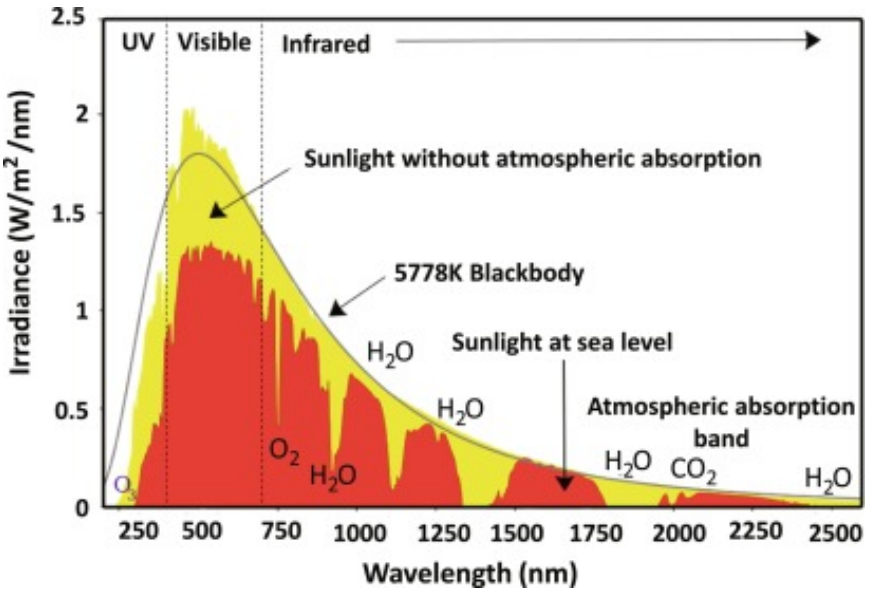

Figure 19. Solar radiation spectrum on Earth. Source: [26].

1. Electromagnetic Waves

The EM spectrum refers to the entire EM radiation frequency range. The EM spectrum ranges from extremely low frequency bands, used for radio communications, to gamma radiation, which has an atom-sized wavelength and a very high frequency [26].

In a vacuum, all EM waves travel at the speed of light, but at a variety of frequencies, wavelengths, and photon energies (Figure 20). The EM spectrum encompasses all EM radiation and is divided into several subranges, or wavelength bands, such as visible light and ultraviolet radiation. The various bands have distinct names due to changes in the behavior of the corresponding waves in terms of emission, transmission, and absorption, as well as their diverse practical uses [27].

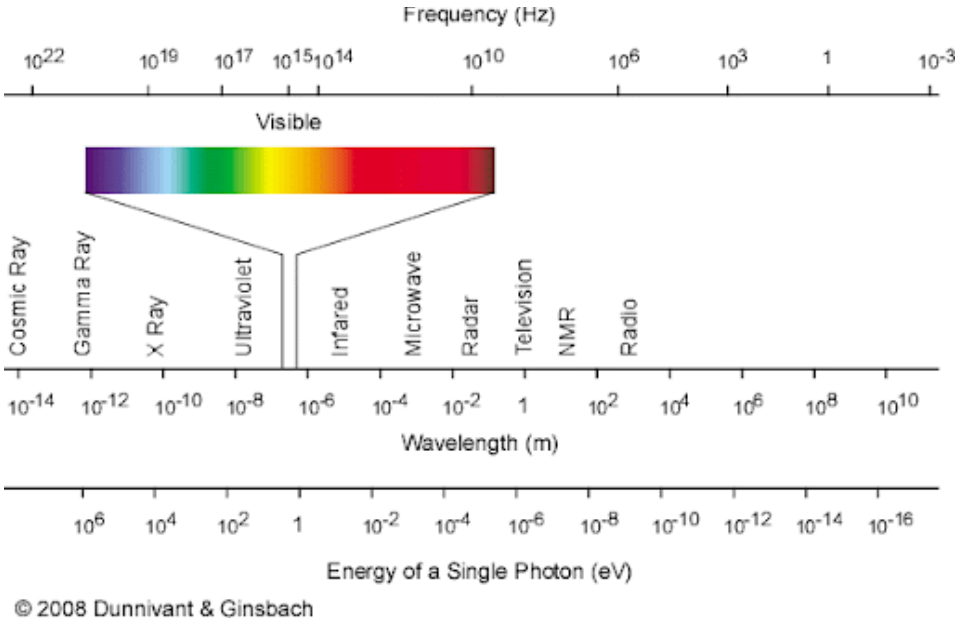

Figure 20. Frequencies, wavelengths, and photon energies. Source: [28].

Three variables are used to describe EM waves: frequency, wavelength, and photon energy. The equations in Figure 21 connect these three physical descriptive properties [29].

$$f = \frac{c}{\lambda} = \frac{E}{h}$$

$$E = \frac{ch}{\lambda}$$

Figure 21. EM waves equations

h is Planck's constant (4.13510–15 eVS), while c is the speed of light. These equations connect the energy of each photon to its wavelength and frequency in EM radiation [29].

2. Solar Radiation

Solar radiation is the term used to describe electromagnetic energy from the sun. The term “sunlight” or “sun energy” is frequently used to refer to it. Solar radiation may be absorbed and converted to usable forms of heat and electrical power through a number of technological advancements. The technological viability and economic viability of these systems are contingent on the amount of solar energy available in a given region, however [28].

Due to the spherical nature of the Earth, the sun shines at a variety of angles on its surface, ranging from 0° (directly overhead) to 90° (just below the horizon). When the rays are vertical and the most direct, the Earth crust absorbs most of the power. As the rays of the sun get more inclined, they become increasingly dispersed as they pass through the atmosphere at an angle. Because the Earth is spherical, the Polar regions have never seen a high sun, and they receive no light at all for a period of the year due to the slanted center of rotation [28].

Because PV systems utilize both direct and dispersed sunlight, the solar resource in the U.S. is abundant. Other technologies may have less capabilities. The quantity of electricity created by any solar device at a given location, on the other hand, is determined by how much of the solar energy reaches it. As a result, solar technologies perform best in the southwestern U.S., which gets the most sun energy [28].

EM radiation travels unaltered in the vacuum of space. When the sun reaches the Earth crust, its power is 1366 W/m^2, with 50% of it outside the visual frequency range range, 40% in the visual range, and 10% in the ultraviolet region. The higher atmosphere, particularly the lithosphere, absorbs ultraviolet radiation. Sunlight is attenuated and refracted as it travels through the several layers of the atmosphere, resulting in fewer photons reaching the Earth. Near the surface, when the sunlight is orthogonal to the Earth surface, the total amount of power is around 1000 W/m^2 [28].

3. Peak Sun Hours

The phrase “peak sun hours” refers to the total everyday solar irradiance in kWh/m^2, as seen in Figure 22. The term “peak sun hours” refers to the quantity of solar

irradiance received at a specific location if the sun shined strongly for a specified number of hours. Since peak radiation from the sun equals 1 kW/m^2, the number of peak sunshine hours is theoretically equivalent to the expected daily solar insolation. For example, a location receiving 8 kWh/m^2 per day can be assumed to get 8 hours of daylight each day at a rate of 1 kW/m^2. Because PV modules are commonly rated at 1kW/m^2, understanding how to calculate peak solar hours is beneficial [30].

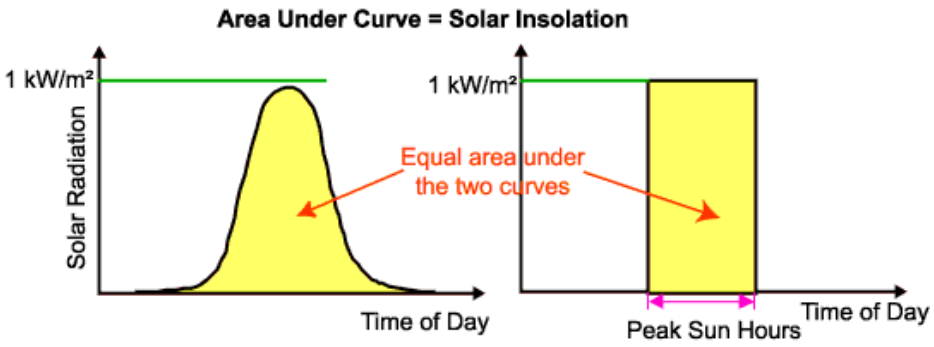

Figure 22. Peak sun hours and solar insolation. Source: [30].

C. PHOTOVOLTAIC THEORY

A PV cell is a type of energy harvesting system that utilizes the PV cell to convert energy from the sun to useable electricity. Although PV cells exist in a variety of forms and dimensions, they always rely on semiconductors to generate an electric current when photons from the sun interact with them [31].

1. General Theory

The semiconductor, which transforms light into energy, is the most important portion of a solar cell. Due to the nature of their electron energy levels, semiconductors may do this conversion. The "valence band" and the "conduction band" are the two main groups of electron energy levels, as shown in Figure 23. The valence band is the most densely packed with electron energy levels, whereas the conduction band is the least densely packed. The term "band gap" refers to the energy differential between the valence band top and conduction band bottom. In a conductor, there is no effective area because

the conduction mechanism is not completely filled, allowing electrons to easily move through into the material. Insulators have extremely large band structures that need a great deal of energy to overcome, preventing electrons from flowing from the valence to the conductive band. In semiconductors, on the other hand, the conduction band is exceptionally tiny, permitting some electrons to transition to the bandgap with only a trace of energy [32].

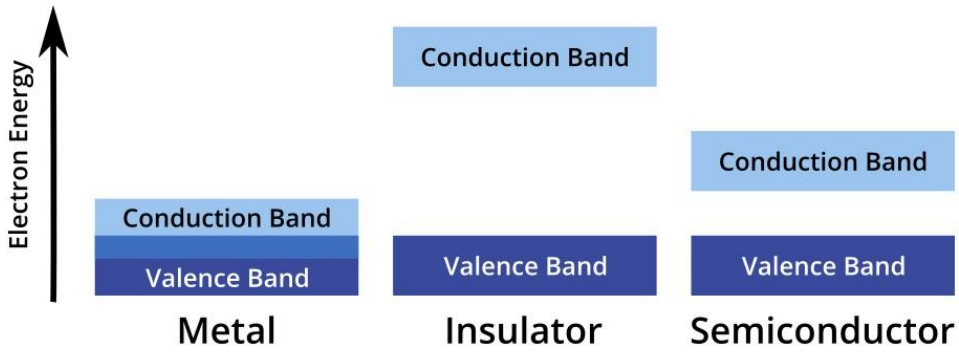

Figure 23. Metals, insulators, and semiconductors showing their own set of energy bands. Source: [32].

Due to their tiny band gap, some semiconductors may create energy from light. The semiconductor absorbs a photon with an energy (E) larger than the band gap, allowing an electron to migrate from the valence band to the conduction band, as seen in Figure 24. This is referred to as "excitation." The valence band is now vacant, as the electron has moved to the conduction band. This is referred to as a "hole," and it behaves similarly to an electron in a bandgap (albeit with positive charge). The excited electrons and gap are coulombically bonded in a state dubbed an "exciton" due to their opposing charges [32].

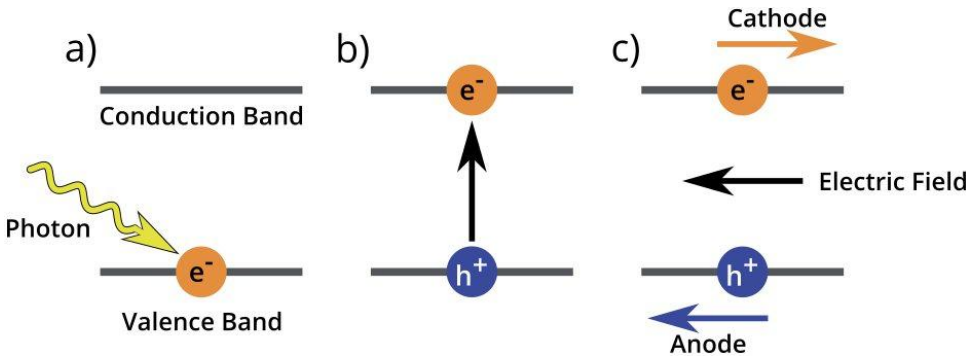

Figure 24. The fundamentals of a solar cell's operation. Source: [32].

2. PV Cell Layering

As seen in Figure 25, a solar cell is made up of several layers of different materials [33], each having its own function. In a solar cell, the most crucial layer is the carefully handled semiconductor layer. It is made from a combination and is responsible for converting the sunlight from light into electrical energy via a process called the PV effect. A layer of conducting material runs along both sides of the semiconductor, collecting the generated power. The last layer is an anti-reflection layer, which allows light arriving at a wide variety of angles to enter the cell. Due to the inherent reflecting nature of all semiconductors, scattering can be severe. To minimize the quantity of sun energy reflected off the exterior of the cell, one or maybe many layers of an anti-reflection layer can be added [31].

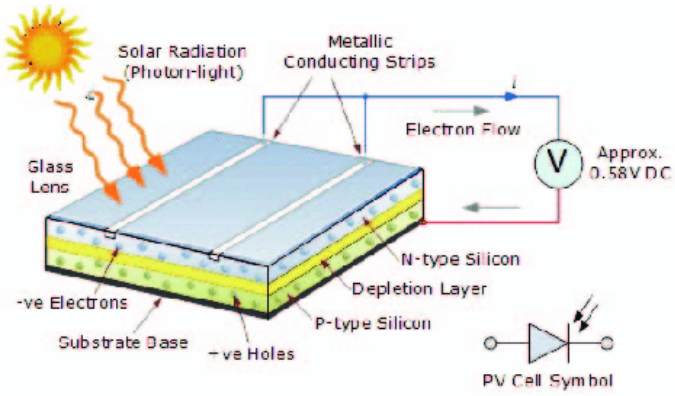

Figure 25. Diagram of a PV cell. Source: [34].

3. Semiconductors

A semiconductor is a silicon-based material that conducts electricity better than an insulator, such as glass, but not as well as a pure conductor like copper or aluminum. The insertion of impurities, known as doping, can change the conductivity and other characteristics to match the unique demands of the electronic component [35].

The amount of energy needed to move an electron from the innermost, valence, electron line to a free state in the bandgap distinguishes semiconductors from conductors and insulators. The band diagrams seen in Figure 26 illustrate various energy levels graphically. Insulators have a band structure more than or equal to five electron volts (eV), conductors have no band gap, and semiconductors fall somewhere in between [6].

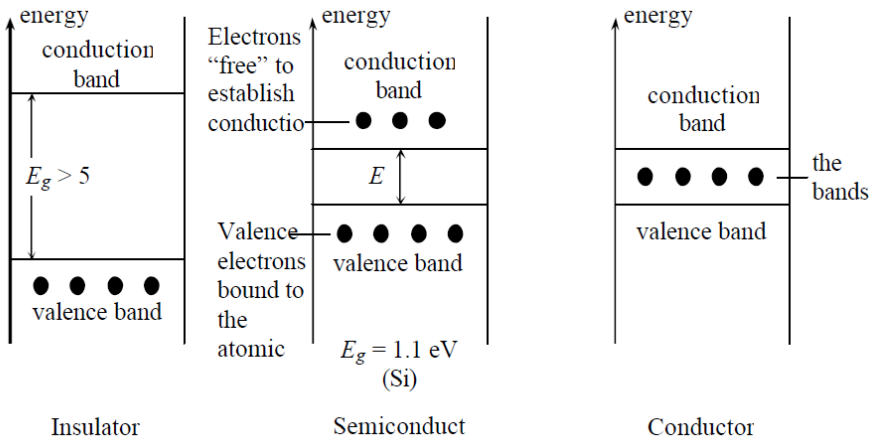

Figure 26. Insulators, semiconductors, and conductors have different energy bands. Source: [6].

Covalent bonds are employed to fabricate semiconductors with stable, crystalline structures. Every atom must have four valence electrons to complete the lattice. A "hole" represents the lack of an electron and thus has a polarity opposite that of the electron but a charge of the same magnitude.

The Fermi level of a material as shown in Figure 27 is defined as the excess of electrons or holes in the band diagram. An electron "donor" is an element containing more than four valence electrons.

Because the additional electrons raise the Fermi level above the center of the band gap, the material is referred to be an "n-type" semiconductor. The term "acceptor" refers to an element having fewer than four valence electrons, and the resulting material contains more holes than electrons. Due to the presence of a significant number of holes, the Fermi level is lowered underneath the center, leading to a "p-type" semiconductor [6].

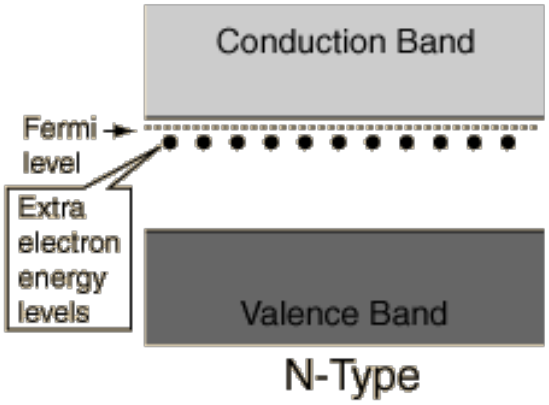

Figure 27. The Fermi level. Source: [36].

4. P-N Junction

A p-n junction is formed when n-type semiconductor material is brought into contact with p-type semiconductor material, as seen in parts B and C of Figure 28. The holes on the p side are referred to as majority carriers due to their predominance as carriers. On the p side, a few electrons will be created energetically; these are referred to as minority carriers. On the n side, electrons are the majority carriers, while holes are the minor carriers. There are no free charge carriers in a spot near the junction. In this place, the source/drain functions as an insulator [37].

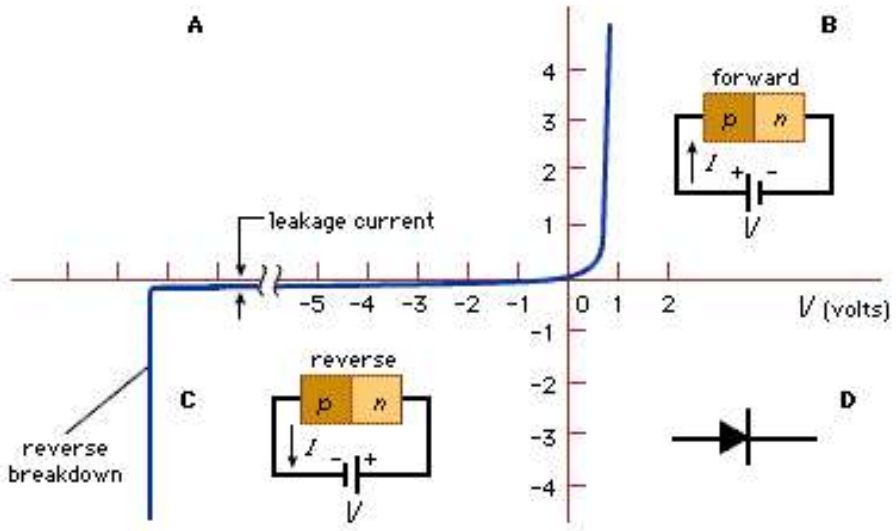

Figure 28. Characteristics of the p-n junction. Source: [37].

The essential property of p-n junctions is their alignment. Section A of Figure 28 illustrates the general properties of a perfect silicon p-n junction [37]. When one applies a forward bias to such a p-n junction a positive power supply is connected to the p-side relative to the n-side, as shown in section B of Figure 28 [37]. Most of the electric charge traverses the junction, allowing for high current to flow. On the other hand, when a reverse voltage is provided, the charge carriers created by impurities flow out from the junction in opposite directions, resulting in a small flow of current [37].

When the reverse bias is raised, the leakage current stays low until a critical voltage is reached, at which time the flow rapidly increases. The name "junction breakdown" refers to this abrupt rise in current, which is frequently a nondestructive process when the accompanying energy dissipation is kept below acceptable limits. Although the applied forward voltage is normally less than one volt, the reverse essential voltage, sometimes referred to as the terminal voltage, can range from less than a volt to hundreds of volts, depending on the junction impurity level and other device parameters [37].

5. Solar Cells

When a photon with an energy slightly greater than the band gap of the material collides with an atom, it may release an electron-hole pair, generating an electron and a

hole in the semiconductor that previously did not exist, as seen in Figure 29. The electron possesses sufficient energy to cross the bandgap. Due to the presence of a p-n junction in the device, electrons can be transported downward toward the n-type surface. A similar hole is pushed toward the p-type side of the solar array, showing the direction of current flow [6].

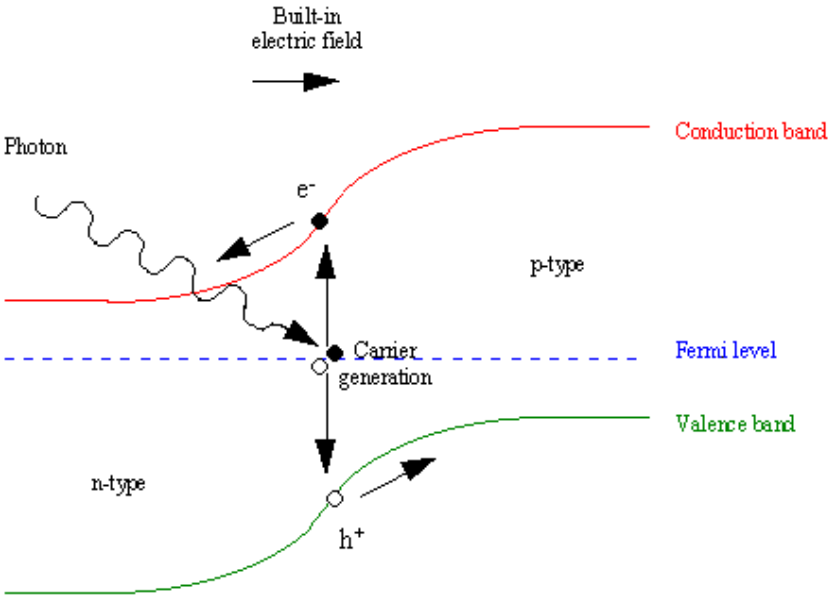

Figure 29. A schematic of photovoltaic bands. Source: [6].

Because of the interior formation of an electron-hole pair, the activated solar cell current travels the opposite direction of the forward-biased p-n junction current [6]. As a result, the typical current–voltage (I–V) resulting from a solar cell is not in the same block as that of a normal diode. This link is illustrated succinctly in Figure 30.

Although the voltage level is almost equal to the junction inherent potential, the short fault current is the highest possible given the prevailing sunshine conditions [6]. The "knee" on the graph indicates the point at which the combination of the working voltage and current of the cell is greatest [6]. Although Figure 30 represents a negative current, subsequent images will depict solar cells with a positive current, following the more conventional I-V characteristics paradigm [6].

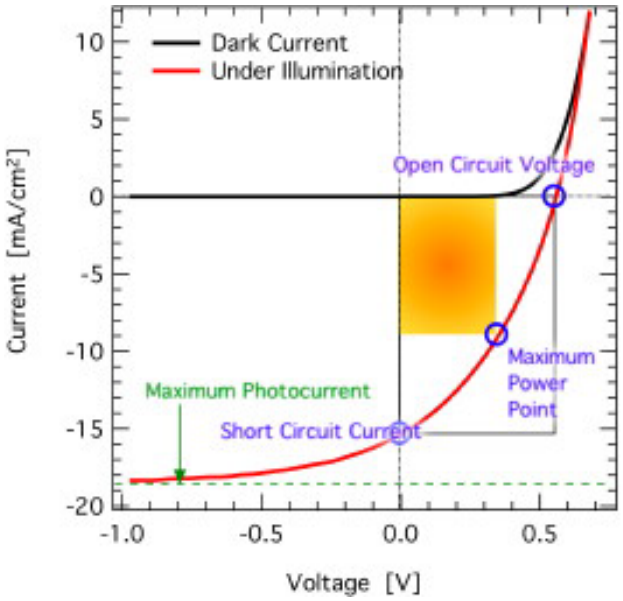

Figure 30. Characteristic curves of light and dark diodes. Source: [6].

6. Solar Cells Efficiency

The efficiency of PV cells is limited by the presence of various factors that limit efficiency. Fundamentally, a silicon semiconductor is incapable of converting 1/4 of the energy production that reaches the Earth to energy. The band-gap energy is the lowest absorption coefficient required to remove an electron from a crystalline structure, as defined by semiconductor physics. When photon energy is less than the bandgap energy, latent heat is collected. The bandgap energy of silicon is 1.12 electron volts. Due to the broad energy range of solar photons, a part of the incoming solar energy is insufficient to force an electron off in a silicon PV cell. There is still an issue about the amount of light that may be absorbed. Energy that is more than the band-gap energy is transformed to heat. This means that the heat energy is not being used effectively. Not all electrons that are made available will find their way to the metal contact and generate energy. This is because the voltage contained within the semiconductor is insufficient to accelerate some of them. Silicon PV cells have a theoretical efficiency of roughly 33%. There are a variety of ways for increasing the efficiency of PV cells, each of which has a cost. Increasing the purity of the semiconductor, utilizing a more efficient semiconductive element such as gallium arsenide, adding more layers or p-n junctions to the cell, or concentrating the energy of the

sun via focused photovoltaics are just a few of these ways. On the other hand, PV cells degrade with time, providing less energy as a consequence of various of factors such as ultraviolet rays and climate cycles [31]. According to a detailed assessment published by the National Renewable Energy Laboratory, the average rate of deterioration is 0.5% each year [38], as shown in Figure 33 from [39].

The ratio of solar cell maximum output power to the available input incident power is the efficiency of a solar cell or solar panel. The efficiency of a solar cell is defined in Figure 31 [29].

$$\eta = \frac{MP}{P_{input}}$$

Figure 31. Solar cell efficiency. Source: [28].

Where "n" is the efficiency of a solar cell. Because the input power is measured in W/m^2, it is important to scale the power to the array size [29].

A solar cell theoretical maximum output power is OC SC V I, and the fill factor is the ratio of the MP point to the theoretical maximum. The theoretical maximum equation is shown in Figure 32 [29]. Figure 33 shows the history of solar cell energy efficiency conversion research [29]. The I-V curve's maximum power point (Pmax) is shown in Figure 34.

$$FF = \frac{MP}{V_{OC} I_{SC}}$$

Figure 32. Theoretical maximum. Source: [29].

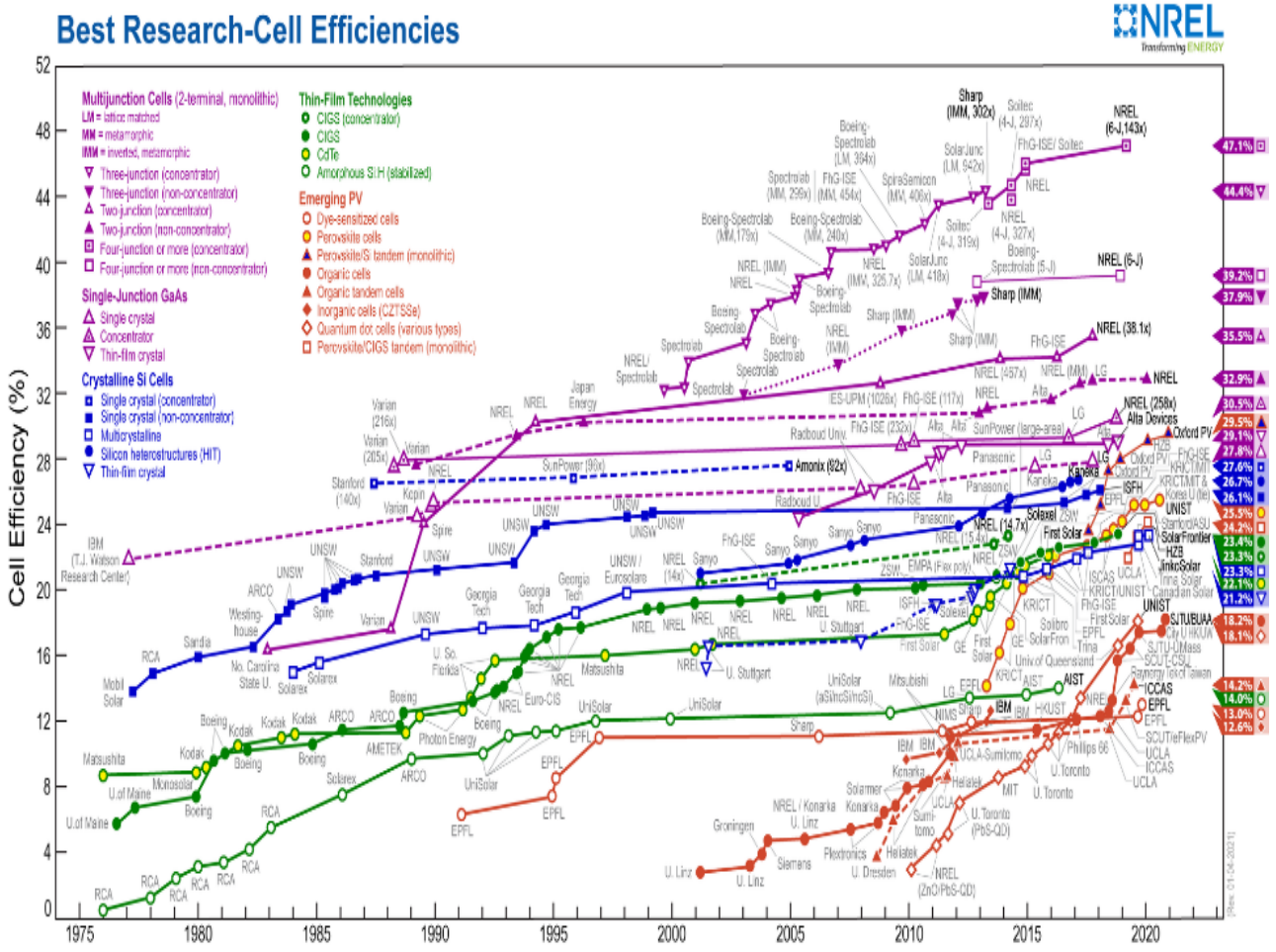

Figure 33. Since 1976, researchers have reported on the efficiency of solar cell energy conversion. Source: [39].

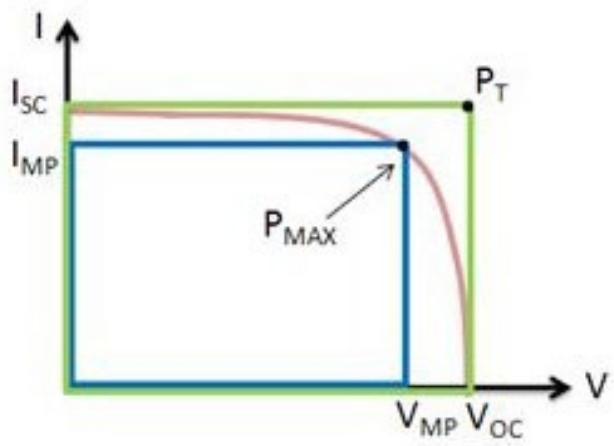

Figure 34. Fill factor I-V curve. Source: [6].

7. Types of PV Cells

A PV cell can be constructed in a variety of ways and using a variety of materials. Although silicon (Si) is by far the most often used semiconductor in commercial PV modules, other materials such as gallium arsenide (GaAs), cadmium telluride (CdTe), and CIGS are also employed. Solar cells are available in two types: rigid crystalline structures (Si, GaAs) and thin-film solar cells (Si, CdTe, CIGS). The two varieties of crystalline PV cells are monocrystalline and polycrystalline [31].

As the names suggest, monocrystalline PV cells have a homogenous or single crystalline structure, while polycrystalline PV cells have various or diversified crystal structures. Solar cells can also be classified according on their layers or "p-n junctions." While the majority of commercial PV cells are single-junction, multi-junction PV cells have been developed that provide greater efficiency at a higher cost [31].

a. First Generation

Silicon is the most researched element, which enables it to get most of the greatest results (with an optimal efficiency of 26.1%), becoming the first material to reach the commercial sector. As a result, silicon is the predominant photoactive material used in solar panels on UAVs (Figure 35). Silicon has a 1.1 eV band structure, which enables it to absorb a significant amount of solar radiation. Due to the fact that this value is less than the optimal

band gap (1.34 eV), energy is lost during photon absorption. Additionally, the conduction band is angled, which reduces adsorption efficiency and necessitates the use of rather thick panels to properly absorb sunlight. Silicon has a high dielectric constant of 11.7 [31].

Figure 35. Silicon solar cells on UAV

b. Second Generation

(1) Gallium Arsenide

At 29.1%, gallium arsenide (GaAs) has the greatest PV efficiency of any semiconductor. GaAs is more favorable because the straight conduction band of 1.43 eV enables it to absorb more light with fewer layers and converting less energy to heat. Furthermore, GaAs outperforms silicon in terms of electron transport parameters. However, it is costly, limiting its usage to space applications [32].

(2) Cadmium Telluride

Cadmium telluride (CdTe) is a 22.1% efficient thin-film PV material. CdTe has the same band gap as GaAs, 1.44 eV, and hence shares the same advantages as GaAs: high permeability in thin films and low photon power loss. Moreover, this element is bendable, which enables industrial PV power to be less expensive than silicon and to have far shorter charging periods. Despite its advantages, there are a few disadvantages: Because cadmium

is very deadly and tellurium is uncommon, the viability of this technology is now in doubt [32].

(3) Copper-Indium-Gallium Selenide

With a high efficiency of 23.4%, CIGS devices performed similarly to CdTe devices. CuInxGa(1-x)Se2 is the chemical formula for the molecule, with x ranging from 0 to 1. The band gap of the material may be adjusted between 1.0 eV (pure copper indium selenide) and 1.7 eV (pure copper gallium selenide) due to the tunability of the chemical structure. CIGS cells, like GaAs cells, are costly to manufacture, however, resulting in solar panels that are not competitive with existing Si commercial technology. Furthermore, indium, like tellurium, is extremely scarce, limiting the long-term promise of the technology [32].

c. Third Generation

(1) Dye-Sensitized

Organic dyes are used to absorb light in dye-sensitized PV modules, as seen in Figure 36. (DSSCs). The dyes are applied to an oxide superstructure immersed in a liquid electrolyte (often iron dioxide). Following absorption of light by the dyes, the excited electron is transported to the metal framework, while the hole is transferred to the electrolyte. At the electrodes, the particles can be gathered. While these cells lose effectiveness when compared to inorganic devices, they can be significantly less expensive because of their roll-to-roll printing, semi-flexibility, and semi-transparency. Due to the temperature stability of a liquid electrolyte, however, there are still issues connected with its use [32].

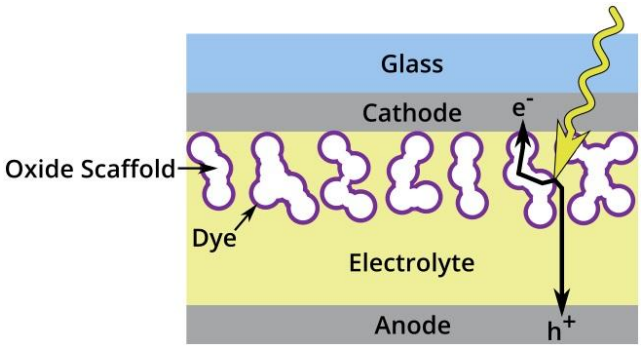

Figure 36. A dye-sensitized solar cell's structure and operation

(2) Organic

Organic solar cells are photoactive devices that utilize organic semiconductor materials such as polymers or organic chemicals. This method has an efficiency of 18.2% to date. These cells operate in a manner similar to that of inorganic devices [32]. On the other hand, organic semiconductors have dielectric loss characteristics, implying that the exciton generated cannot be thermally separated. Rather than that, the exciton must be moved to an interface with a material whose energy level is offset from the photon binding energy [32]. The electron (or hole) is then able to go to the other material, dividing the exciton and collecting the electric charge [32]. Because excitons may only diffuse for about 10 nm before the electron and hole recombine, organic PV cell thickness, structure, and, ultimately, performance are limited [32]. Despite this, these devices have a number of benefits over inorganic devices, including lower material costs, lighter weight, stronger and more tunable absorption properties, flexibility, and the ability to be produced utilizing roll-to-roll printing processes. Organic compounds now face stability concerns as a result of photochemical degradation [32].

(3) Perovskite

Perovskite solar cells have a light-absorbing layer composed of perovskite minerals (materials having the crystal structure ABX3). Perovskite solar cells, as shown in Figure 37 from [32], are a new technique in the field, having been used in a PV system for the first time in 2006 (achieving 2.2%). Due to the publishing of a seminal work in which a 10.9% efficiency was obtained, 2012 is considered the birth year of the discipline.

Perovskite solar cells have increased their peak efficiency to 25.5% since then, making them the fastest-improving solar technology. Strong tunable absorption characteristics and ambipolar charge transfer are two of the outstanding qualities of this material [32].

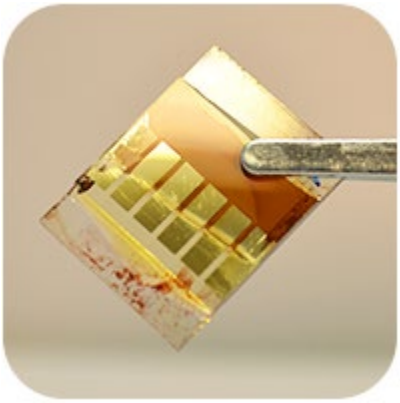

Figure 37. Perovskites solar cells. Source: [32].

Table 4 shows a comparison of the highest efficiencies of solar cell types as of 2021.

Table 4. A solar cell made of perovskite. Source: [32].

Solar Cell Type	Highest Efficiency (Last updated 19/02/2021)
Monocrystalline silicon (mono-Si)	26.1%
Polycrystalline silicon (multi-Si)	23.3%
Amorphous silicon (a-Si)	14.0%
Monocrystalline gallium arsenide (GaAs)	29.1%
Cadmium telluride (CdTe)	22.1%
Copper indium gallium selenide (CIGS)	23.4%
Dye-sensitised (DSSC)	13.0%
Organic (OSC)	18.2%
Perovskite (PSC)	25.5%

8. Copper-Indium-Gallium Selenide Solar Cells

CIGS is a semiconductor material composed of copper, indium, gallium, and selenium. CIGS solar cells have an extraordinarily high absorption coefficient of more than 105/cm for photons with an energy of 1.5 eV and higher. [40].

CIGS solar cells (often referred to as CIS cells) are a kind of thin-film solar cell that convert solar energy to electrical energy. Copper, indium, gallium, and selenium thin films, as shown in Figure 38 from [36], are placed on a plastic or glass backing and equipped with front and rear electrodes for current collection. In comparison to other semiconductor materials, a substantially thinner covering is required due to the high absorption coefficient and intensive absorption of sunlight by the material [40].

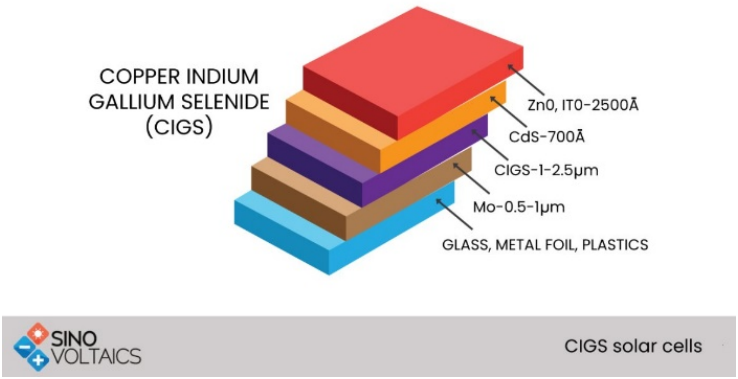

Figure 38. Copper-indium-gallium selenide representation. Source: [39].

Thin-film solar modules based on CIGS are an efficient alternative for major commercial solar panels. CIGS is a highly flexible material that can be manufactured in a variety of ways and applied in a variety of ways. On a range of surfaces, such as glass, metal foils, and polymers, CIGS may be deposited. Metal foils and polymers may be advantageous in applications that need lighter-weight or more flexible modules [41].

D. DC-TO-DC CONVERTERS

The power controller on the UAV is a DC-to-DC converter that allows the solar panel voltage output to be adjusted or decreased to fulfill a load requirement. The

electronics required for these adaptations are described in the sections below [29]. DC-DC converters are frequently used to effectively provide a regulated power supply from an unregulated source especially when the load varies. DC-DC converters are high-energy conversion circuits that convert voltage fluctuations to regulated direct current voltages through the use of high-frequency switching and inductors, transformers, and capacitors [42].

A boost converter is a voltage "step-up" converter. Boost converters consist of a switch, including a diode or a transistor, and a storage battery, such as a capacitance or an inductance. The rationale behind this gadget is that inductors resist current change [29]. A basic boost converter circuit is shown in Figure 39 from [43].

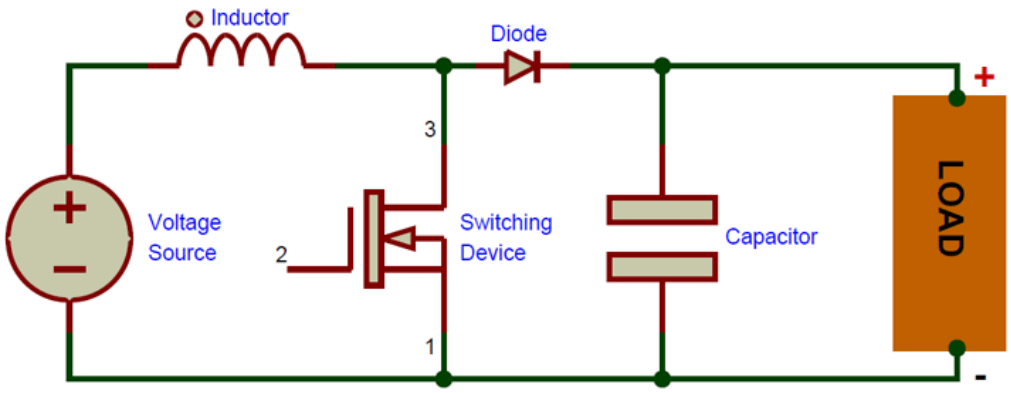

Figure 39. Circuit diagram of a common boost converter. Source: [43].

In [29], Alexis Harvey shows the load was disconnected from the circuit when the circuit is switched. In Alexis' study, the inductor magnetic field can be employed to store energy supplied by the supply voltage. When the switch is opened, the load is rapidly reintroduced into the circuit, causing a rise in either voltage or current [29]. Furthermore, the study demonstrated that the inductor resists the increased current demand and hence shows to the charge as a supply voltage series—connected with the input source, thereby supplying the load with the needed higher voltage. If the switch is cycled quickly, the inductor rarely completely discharging, and the load continues to perceive the voltage as

supply voltage [29]. Additionally, the capacitor linked to the load is charged to the enhanced voltage level while the switch is open. When the circuit is completed, the capacitor acts as a voltage source for the load [29].

The duty cycle of a switch is defined as the ratio of open to closed time. The duty cycle is always less than one since it indicates the percentage of time the circuit is active vs. time it is off [29]. This is shown in the equation in Figure 40.

$$D = 1 - \frac{V_i}{V_O}$$

Figure 40. Representation of the duty cycle. Source: [29].

The equation in Figure 41 [29] is transposed; the output voltage always seems to be greater than the input voltage [29]:

$$V_O = \frac{V_i}{1 - D}$$

Figure 41. Representation of the equation rearranged.
Source: [29].

A buck converter is a DC-to-DC power converter that decreases the voltage from the input (supply) to the output (while drawing less average current) (load). This is a form of switched-mode power supply that typically appears to contain two semiconductor materials [44]. Figure 42 shows an example of a buck converter.

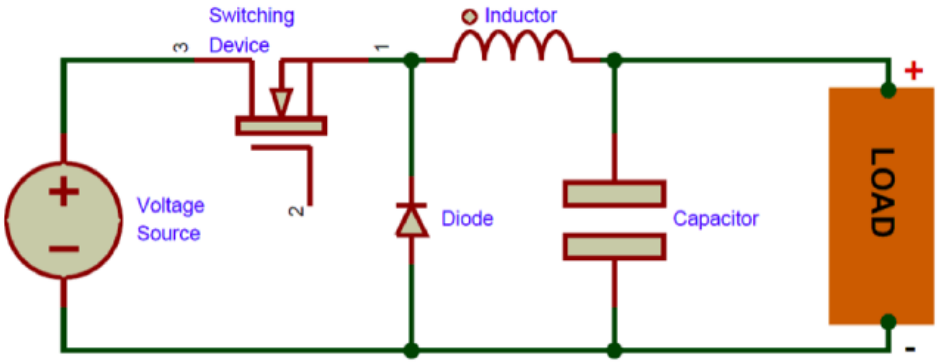

Figure 42. Buck converter. Source [43].

The circuit is "off" while the switch is open, and there is no current flowing through the load. Current begins to flow towards the load when the switch is closed; nevertheless, the inductor opposes this rise in current. To sustain the energy situation, the voltage on the inductor load side decreases. Because the inductor is connected to a capacitor, if the switch is turned off before the inductor magnetic field has built up to its full value, the load should always experience a voltage smaller than the source voltage [29]. The duty cycle may be used to characterize the buck voltage relationship, as shown in the equation in Figure 43.

$$V_O = DV_i$$

Figure 43. Relationship of the buck voltage. Source: [29].

E. CONCLUSION

For optimal PV use, a combination of disparate yet critical factors is necessary. To begin, much sunshine is necessary. The cells should be positioned so that they capture incoming light at the most normal angle possible. The cells should be positioned in such a way that their voltage and current characteristics are utilized to meet power requirements,

and they should function within the same wavelength range as the incident light. In terms of cost and weight, CIGS cells are the most efficient solar cells available. As seen in Figure 43, this determination is a snapshot in a dynamic field. Solar cell performance and cost may improve in the future, making them a more attractive power gathering choice. Once energy is obtained, it must be utilized immediately or stored for later use. The following chapter complicates the system even further by demonstrating the critical role of battery technology in predicting power requirements and designing a solar array.

V. COPPER-INDIUM-GALLIUM SELENIDE

A. INTRODUCTION

In [45], G. Harper shows that the CIGS solar cell, also known as the complete copper-indium-gallium selenide solar cell, is a form of TFPV panel that receives sunlight and converts it to electricity using CIGS semiconductor layers. Harper mentioned that despite the fact that CIGS solar cells are still in their infancy in terms of widespread application, they may be created utilizing a process that has the potential to decrease the price of PV functionalization. As CIGS product performance, uniformity, and reliability increase, the technology has the potential to rapidly grow market share and become "disruptive" [45]. Additionally, considering the risks associated with cadmium mining and usage, CIGS solar cells have fewer environmental concerns than cadmium telluride solar cells [45].

B. CIGS SOLAR CELL FEATURES

A thin sheet of copper indium selenide and copper gallium selenide, as well as a tiny quantity of sodium, are used in CIGS solar cells, as shown in Figure 44 from [6]. Due to the unequal band structure of the two materials, the CIGS film functions as a narrow-band gap semiconductor, forming a heterojunction. The thin-film cell back surface contact is produced by mounting it on a substrate such as soda-lime glass, metal, or a polyamide film. When a nonconductive substrate is employed, a conductor such as molybdenum is used. For light to enter the cell, the front surface contact must be both conductor and transparent. To obtain the requisite ohmic contact, materials such as indium tin oxide, doped zinc oxide, or, more recently, complex organic films based on nano-engineered carbon were utilized [45].

The translucent front ohmic contact allows light to pass through and is captured by the CIGS layer in the cells. The electron-hole pairs are generated in this region. A "depletion region" arises at the heterojunction of the p- and n-type materials on the cadmium-doped surface of the CIGS cell. This isolates the electrons from the holes and allows for the transmission of an electrical current. In 2014, laboratory studies revealed

that a CIGS cell with a revised surface morphology attained a record efficiency of 23.2%. Commercial CIGS cells, on the other hand, have a lower conversion efficiency, with the majority of modules converting at roughly 14% [45].

CIGS films are frequently deposited onto a substrate in a vacuum during the manufacturing process, using either an evaporative or a sputtering approach. Copper, gallium, and indium are sequentially deposited and annealed with a selenide vapor to generate the final CIGS structure [45]. Without a vacuum, deposition can be accomplished by the use of nanoparticles or electroplating, but these techniques will require more study to be economically viable on a large scale [45]. Novel manufacturing techniques are being developed that are more analogous to printing than to conventional silicon solar cell manufacturing [45]. In one way, a printer uses semiconducting ink droplets to print on aluminum foil. After another printing step deposits additional layers and the front contact on top of that layer, the foil is then divided into sheets [45].

Figure 44. Structure of a typical CIGS cell. Source: [6].

C. CIGS SOLAR CELLS EFFICIENCY

Solar Frontier established record lab efficiencies of 23.4% in 2019 using Cu(In,Ga)Se2 (CIGS) solar cells, making them one of the most popular thin-film technologies [45]. The straight bandgap and high absorption coefficient of the CIGS material make it ideal for solar panels. As shown in Figure 45, efficient solar absorption may be obtained in CIGS layers as thin as 1 µm; this is 100 times thinner than a silicon

crystalline solar cell. This is encouraging news for the creation of high-efficiency solar cells that consume little materials. Another significant property of this material is its ability to exhibit good optoelectronic properties over a broad compositional range. Additionally, the bandgap of CIGS material synthesized by alloying CuInSe2 with varying amounts of Ga may be adjusted. Ga concentrations are often x=3 in high-efficiency CuIn1-xGaxSe2 devices. To widen the bandgap, the alloy can be supplemented with other elements such as Ag or S. [45].

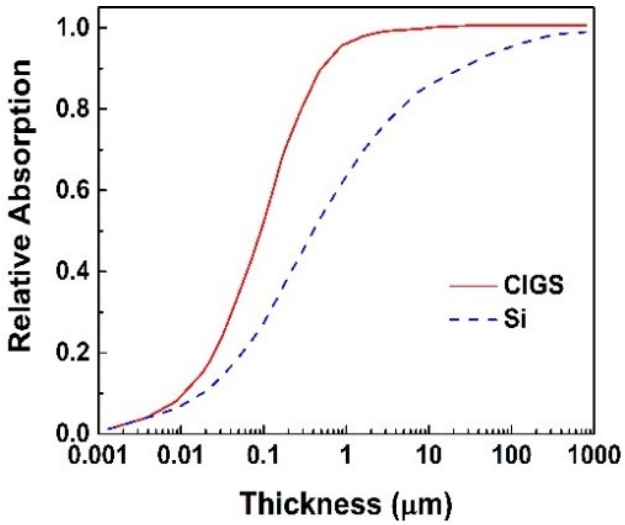

Figure 45. Relative absorption of conventional Si and CIGS solar cells is compared. Source: [45].

Ongoing research and development have resulted in certified AM1.5 cell performance of up to 22.6% for CIGS. Despite its high efficiency, CIGS-based PV technology has not yet realized its maximum potential. If all loss sources were handled concurrently, a level of efficiency of roughly 30% would be technologically possible [33].

The 22.6% efficiency of CIGS solar cells set a global record for any thin-film technology, surpassing that of multicrystalline silicon (21.9%). It was created using a layer sequence identical to that is shown in Figure 46.

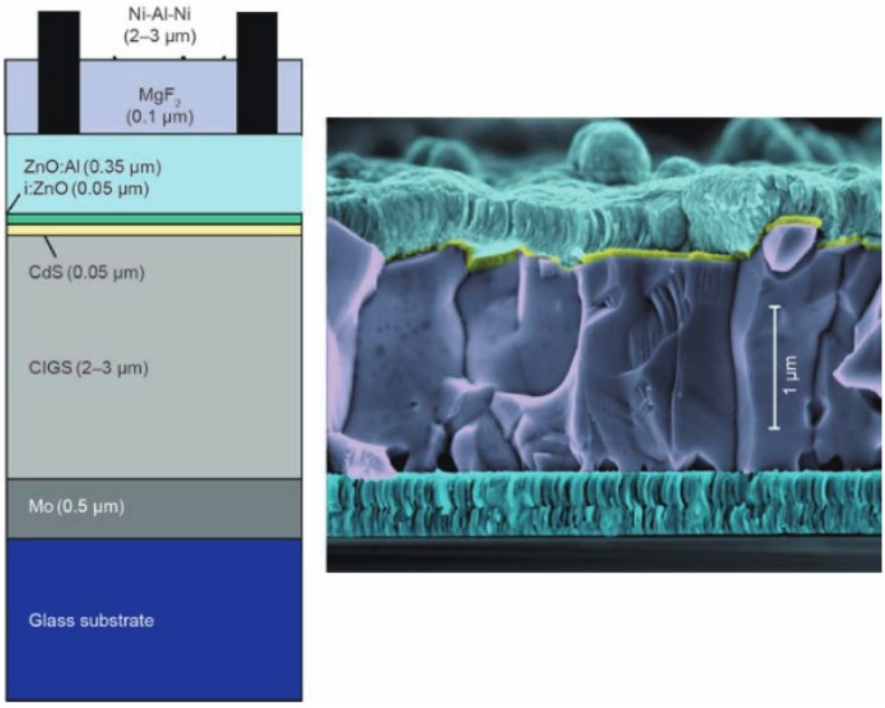

Figure 46. Cross-section scanning electron microscope picture of a conventional CIGS solar cell (right) and a schematic construction of the solar cell (left). Source: [33].

By focusing on efficiency rather than cost, a very high-efficiency cell with a somewhat thicker CIGS absorber layer was produced. At ZSW, these operations are carried out on a dedicated high-efficiency cell production line, with each step being rigorously calibrated. Recent efficiency gains of over 21% were enabled by a significant modification made following the CIGS growth phase. The so-called "post-deposition treatment" involves evaporating alkali fluorides in a selenium (Se) environment to alter the surface composition, lowering the copper and gallium (Cu) concentrations while increasing the alkali element content. Potassium (K) and rubidium (Rb) are two such elements. This treatment of the CIGS–CdS interface has an effect on the p–n junction's quality, and hence on the device's performance. The post-deposition treatment approach significantly increases open-circuit voltage, most likely due to decreased charge carrier recombination at the interface region [33].

D. BENEFITS AND PRODUCTION

The following are some of the advantages of CIGS solar cells:

- High absorption: Because this material has a narrow bandgap, it absorbs a substantial portion of the solar spectrum; it is the most efficient thin-film technology known.
- Tandem design: Due to the configurable bandgap, tandem CIGS devices are possible.
- Protective buffer layer: Grain boundaries act as a protective buffer layer, limiting surface recombination and permitting the use of films with grain sizes of less than 1 micron in device production.

The 1980s saw the development of two low-cost deposition processes that result in the highest device and module efficiencies. These are the methods [46]:

- In a process referred to as co-evaporation, in a high-vacuum environment, precursor elements are permitted to sublimate and are then deposited on a heated substrate.
- The processes of the precursor reaction, in which a Cu and In/Ga precursor is laid down at a low temperature using one of various methods, including sputtering or electroplating. The CIGS films are then formed by a reactive annealing process in a Se compound, such as hydrogen selenide (H2Se) or gaseous selenium (Se). This is also known as two-stage deposition; a three-stage deposition variation of this technology is also widely employed.

THIS PAGE INTENTIONALLY LEFT BLANK

VI. MAXIMIZING THE CONSTRUCTION OF POWER INTERFACE CIRCUITS

A. INTRODUCTION

The circuit that connects the solar panel and the battery is vital in ensuring the greatest amount of electrical energy is provided according to the UAV requirements. The operational voltage range of the battery and its individual cells, as well as the characteristic curve of the PV system, are the key drivers of these selections. This chapter covers the operation of MPPTs, EEMS, and battery balancers as they pertain to this research.

B. MAXIMUM POWER POINT TRACKERS

MPPT is an electrical device that governs the operation of solar modules in order to maximize their energy output. MPPT is not a manual monitoring system in which modules are "physically shifted" to direct their energy more directly toward the sun. MPPT is a completely electronic system that changes the electrical operating point of the modules to maximize the available power. Extended battery charge current allows for the use of the additional power obtained from the modules. While MPPT can be used in conjunction with mechanical tracking, the two are not synonymous [47]. The operational point on the I-V curve, as shown in Figure 47, influences the quantity of energy that a solar cell can produce [47].

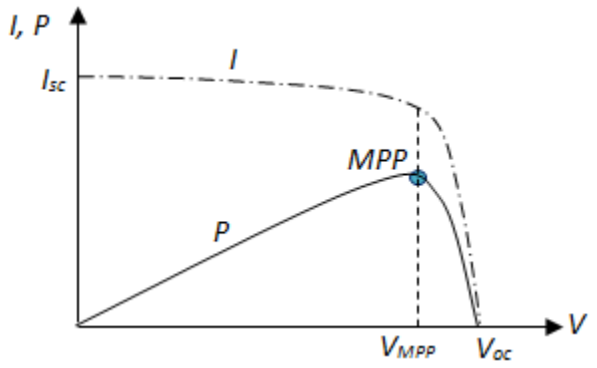

Figure 47. PV array typical I-V and P-V features. Source: [48].

1. MPPT Algorithms

a. Perturb and Observe Algorithm

MPPT methods are used to extract the maximum amount of energy possible from the solar cells in order to get the maximum power point. The MPPT is a voltage-control technique used in PV systems to check whether the system works at peak voltage. To obtain the maximum power, the perturb and observe and incremental conductance MPPT algorithms are utilized [49].

The most typical MPPT approach is perturb and observe, in which the controller modifies the voltage from the PV array by a tiny amount and monitors power. This approach may cause power output fluctuations. The operational point of the solar cells is constantly perturbed by this method, which increases and decreases the conditional parameters. This program compares the output of solar cells before and after disturbance [49].

b. Incremental Conductance

This program calculates the solar cells' instantaneous conductance. To attain the highest power point, this technique increases or reduces the voltage based on the outcome. To forecast the impact of a voltage change, the controller detects incremental changes in PV array current and voltage. This approach involves more computing in the controller, but it is faster at tracking changing circumstances than the perturb and observe method [49].

By comparing the incremental conductance (I/V) to the array conductance (I/V), the incremental conductance technique calculates the highest achievable power point. When both of these parameters are equal (I/V = I/V), the output voltage equals the maximum power point voltage. The controller maintains a constant voltage until the irradiation intensity fluctuates, at which time the procedure is repeated. The incremental conductance approach is based on the finding that $dP/dV = 0$ and $P = IV$ at maximum power [49].

2. MPPT-Enabled Solar Charge Controller

Solar cell voltage and current outputs are directly proportional to the quantity of solar energy they collect. Figure 48 depicts a series of curvatures that illustrate this pattern. Each curve has a point (indicated by a circle) when the power is at its highest. The tip of each curve's is found at the bend of the curve. The MPPT is usually implemented as an integrated circuit that autonomously identifies and analyzes that point to ensure solar cell maximum power production. In turn, the integrated solar charge controller delivers the controlled voltage needed to charge the batteries and power the different onboard loads [50].

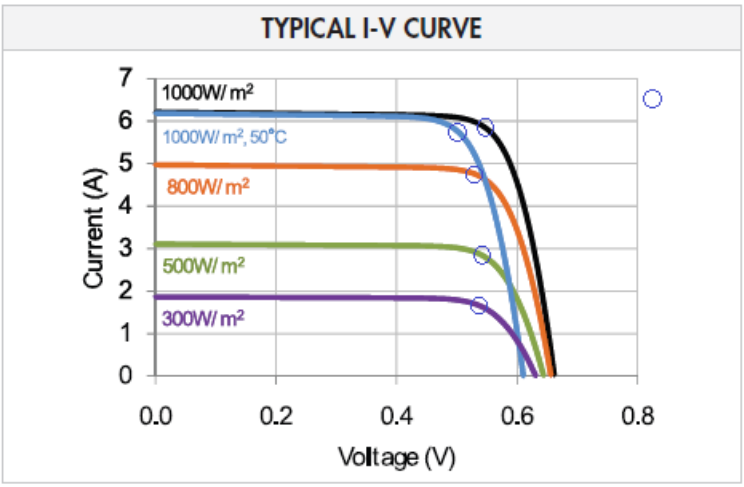

Figure 48. Sun-power solar cell voltage-current curve. Source: [50].

C. ELECTRICAL ENERGY MANAGEMENT SYSTEM

This mechanism optimizes and secures the collection, storage, and distribution of electrical power aboard. It not only accomplishes the usefulness of gathering and storing energy, but it also manages a variety of additional activities, such as [50]:

- Ensuring that the highest amount of energy is extracted from the PV cells
- Producing the charging of the batteries on the UAV

- Preventing anomalous battery behavior such as overloading and draining; regulating current while recharging or draining
- Regulating the charge/discharge of the battery cells
- Forecasting the quantity of energy accessible for safe flight by monitoring current and voltage at every branch of the electrical system

The EEMS includes a solar charge controller as well as a MPPT controller, which harvests the optimum power (voltage and current) from the PV cells. The MPPT device produces a continuous voltage with variable current as its output [50].

Figure 49 shows the typical UAV flight profile. This consists of five distinct phases: takeoff, ascending, cruising, descent, and landing, with “hmax” denoting the flight’s greatest height. The UAV power consumption is relatively constant, sequential, and continuous during each stage [51]. Figure 50 [51] also shows the matching power profile. During the takeoff stage, the power level is around 1 kW, and during the landing stage, the rated power is 600 W [51].

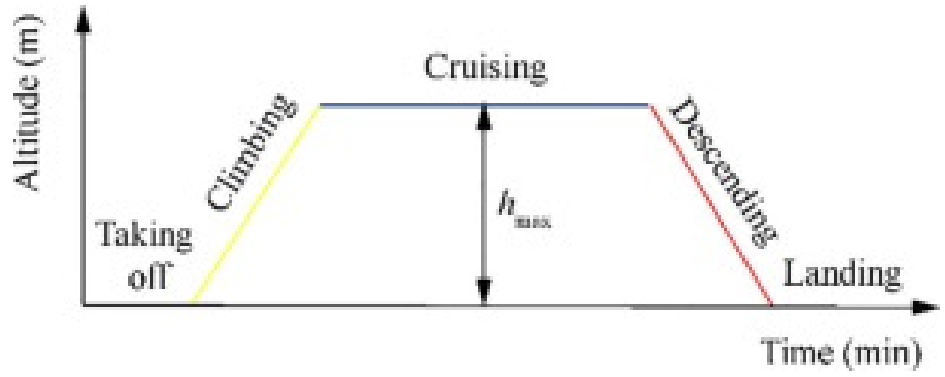

Figure 49. A conventional UAV flight profile. Source: [51].

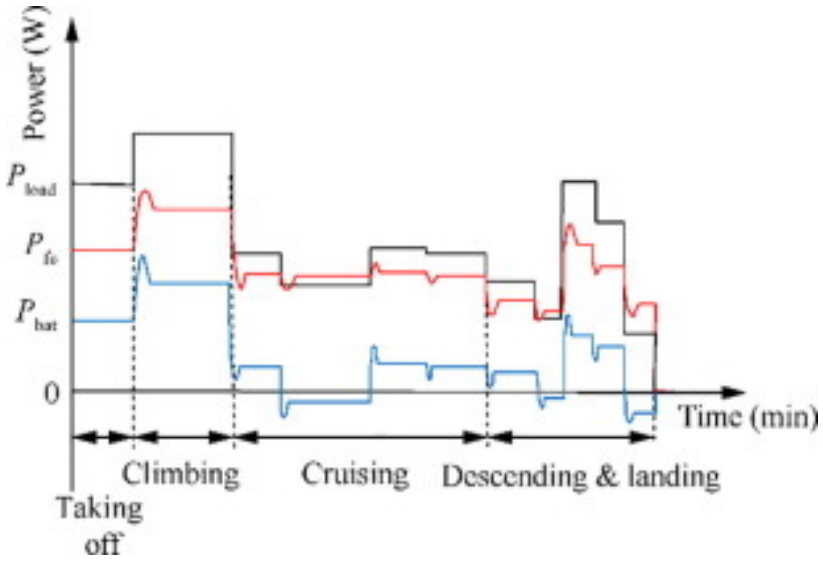

Figure 50. A power profile for a UAV flight. Source: [51].

It can be observed that the load power is highest during the stage of taking off and ascending, and the peak power of the load surpasses the maximum power of each source. As a result, both of them must share the load power of these stages at the same time. The load power during the cruising stage is generally modest and consistent, but the next-level power requirement comes in descending and landing with substantial variability. Conventional passive control systems rely on the inherent power characteristics of each source, resulting in significant energy waste and minimal security, whereas active control methods regulate power distribution through an EMS controller [51].

D. BATTERY BALANCERS

Unlike lead-acid batteries, which need minimal maintenance and are tolerant of neglect, lithium-based batteries necessitate extra caution and vigilance if they are to be reliable and long-lasting. In the worst-case situation, if given enough provocation, a badly maintained lithium battery might spontaneously catch fire [52].

Over time, lithium battery cells will begin to diverge in their state of charge when it is charged and drained frequently. This happens despite the fact that all cells have the same charging and discharging currents [52].

Some cells may be overloaded and others may be undercharged if a battery is repeatedly charged and drained without respect for cell balance. Overcharging destroys cells and shortens battery life, while undercharging prevents the battery from storing the maximum amount of energy possible. Overcharging damaged cells, on the other hand, is a risk factor for ignition [52].

Battery balancers connect to the lithium battery charging ports and monitor the voltage throughout each cell on a regular basis. When the voltage of one cell is higher than the other, the circuitry analyzes the voltages and discharges the over-charged cell at a safe rate until the cells have the same voltage [6].

In a UAV, if the battery is to be charged at low throttle positions, this circuitry is critical to guarantee proper battery balanced. The battery cannot be charged any further if one cell reaches 4.2 V before the others [6].

A precise device that may be used as a hand-held battery verification tool or mounted within a UAV to balance battery cells, while also reporting cell voltages and temperature over the vehicle CAN bus, is a 6S Battery Balancer and is shown in Figure 51.

Figure 51. Monitor and balancer for 6S battery cells. Source: [52].

VII. SYSTEM ANALYSIS

A. INTRODUCTION

At the beginning of this thesis research, we had planned to purchase a Nimbus Pro VTOL aircraft for experimental work. Due to budgetary, supply, and schedule limitations, however, we were unable to acquire one of the vehicles for our project. Instead, we adjusted the scope of our work and proceeded to develop an analytical solution to answer the question of whether the addition of a solar array could extend the mission time of this particular aircraft. The analysis begins with the estimation of the power consumption of the Nimbus Pro VTOL. Since that information is not shared by the manufacturer, we approximated the power consumption based on the limited information available on this aircraft. Factors taken under consideration for our analysis included size, weight, battery type and capacity, the number of motors utilized, and their configuration. We also assumed a typical mission profile with expected power requirements for each phase of the mission. The analysis used realistic flight conditions, such as throttle settings of 85% for take-off, 56.3% for orbiting and maneuvering, and 5% for descent and landing. Those throttle settings are considered typical for each phase of a mission.

After we had obtained an approximate power consumption for the aircraft for a typical mission, we estimated the expected power generated from an array of solar cells installed on the wing of the aircraft. This estimate assumed that the array consisted of CIGS solar cells with an assumed efficiency. The size of the array was based on the estimated surface area available of the single-wing of the Nimbus Pro VTOL. We also assumed a nominal value for the solar irradiance for the location in the north of Peru, as well as the angle between the line of sight to the sun and the solar array normal.

Finally, with estimates of power consumption for the UAV and the power generated by the solar cells, we proceeded to approximate the additional flight time gained by the installation of the solar array.

B. POWER CONSUMPTION

The power consumed by the drone aircraft was not made available by the manufacturer. We were able to approximate this value by considering some of the information that was available, however. Knowing the size and weight of the drone and the capacity of the battery, we could make some assumptions about the motors that would be suitable for the Nimbus Pro VTOL. In addition to the motors, we also made assumptions about payloads, avionics, and actuators that would be required for the aircraft.

1. Motors

Based on the weight of the aircraft and the required thrust for each motor, the Turnigy Aerodrive SK3 2822-1740kv brushless outrunner motor was selected for this analysis. This particular UAV uses five motors. Four are used for the take-off and landing, and only the nose-mounted motor is needed for orbit and maneuvering. From the vendor information, each motor is rated for 115 watts maximum power. An image of the motor is shown in Figure 52.

Figure 52. Turnigy Aerodrive sk3 2822-1740kv brushless outrunner motor. Source: [58].

2. Avionics

For the avionics, we included the following devices: communications tools (transmitter and receiver), GPS, actuators for the flying surfaces, camera, and autopilot. Since the analysis is based on assumptions and calculations of possible results, we have presented in Table 5 the avionics power requirement from the Puma UAV. We have assumed that those values are similar to those that would be used in the Nimbus Pro VTOL.

Table 5. Avionics Puma's power required

System Configuration	Puma's Power Required (W)
Flight control assembly neutral	3.6
Flight control servos active	1.6
Strobe lights on	0.1
Payload installed, off	6
Payload installed, on	0.9 to 1.6

3. Servo Actuators

We used four servo actuators for this analysis, according to the characteristics of this specific UAV. The actuator that we used was the Hi-Tec HK15328D. It requires 500mA at 6 VDC (3 watts). The Hi-Tec HK15328D is shown in Figure 53.

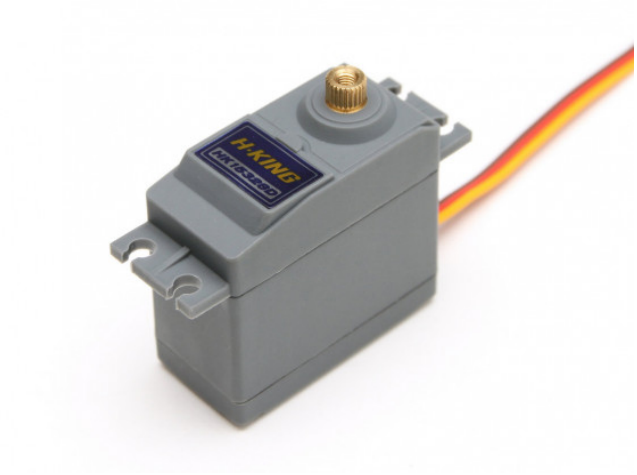

Figure 53. Servo actuators in the Nimbus Pro VTOL. Source: [58].

C. TOTAL ENERGY CAPACITY OF THE NIMBUS PRO VTOL BATTERY

The Nimbus Pro VTOL battery is the Tattu 6S 25000 mAh; it has the following characteristics:

- Voltage (fully charged): 22.8 V
- Capacity: 25000 mAh
- Nominal Voltage: 18.8 V

With the data presented above, we could obtain the total energy capacity of the Nimbus Pro VTOL battery with the following formula [54]:

$$W_{batt} = \frac{E_{full} + E_{nom}}{2} Q_{rated}$$

$$W_{batt} = \frac{22.8v + 18.8v}{2} 25Ah = 520Wh$$

D. BASELINE PERFORMANCE

In this section, we evaluated the baseline performance of the aircraft without the addition of the solar array. Based on the information of the total energy capacity of the Nimbus Pro VTOL battery and also taking into consideration previous calculations of the Raven and Puma motor performance [55], we established the throttle setting for essential phases of a typical mission as shown in Table 6.

Table 6. Average throttle for each mission phase

Mission Phase	Avg Throttle	Used it
Standard Ascent Rate	80–100%	85%
Standard Operating Regime	40–60%	56.30%
Standard Descent and Land	5–10%	5%

Table 7 shows the energy consumed for each phase of mission flight. Beginning with the battery capacity of 520 Wh, each phase of the mission reduced the battery capacity in accordance with the power required and the time period needed for each phase. The throttle settings and times for each phase are also shown in Table 7. These values are also those used previously in analysis of the Puma and Raven UAVs considered in [55]. For the take-off and landing phases, four motors are required, but for the orbit and maneuvering phase, only the nose-mounted motor is needed. Each motor, however, regardless of the flight phase needs 115 watts. For all three phases of flight, the essential avionics, such as radios, servos, and other needed electronics, are lumped together as the payload with a power requirement of 65 watts. Finally, the table includes a residual capacity for the battery of 199.42 Wh. This is an important aspect concerning the use of LiPo batteries. They cannot be discharged to their minimum capacity without causing permanent damage to the battery.

Focusing on the orbit/maneuvering phase, most of the flying time occurred here. Out of the total 100 minutes of operation, 96.36 minutes (1.606 hours) was available for orbit and maneuvering. Additionally, only one motor was required for this phase of flight,

which consumed 115 watts plus 65 watts for the payload. This totaled 180 watts for the orbit/maneuvering phase of the mission.

Table 7. Flight profile

Profile	Time (hr)	Throttle (%)	Power consumed by the payloads (W)	Number of motors used	Total power from the motors (W)	Total Energy consumed (Wh)
Starting capacity of battery						520
Take off and climb	0.022	85%	65	115 watts x 4	460	-11.55
Orbit/maneuvering	1.606	56.30%	65	115 watts x 1	115	-289.08
Descent and land	0.038	5%	65	115 watts x 4	460	-19.95
Total power left	1.667					199.42

E. CONCLUSION OF POWER CONSUMPTION

In this section, we determined that the power consumption of the Nimbus Pro VTOL was approximately 180 watts for the orbit/maneuvering phase. We recognize that this is not an exact value, but it is the best estimate we have based on the available information. Since we had to determine it based on an evaluation of the number of motors used and the power consumed by the payloads in that specific time, values that are not completely exact, and since that fabrication company never provides such kind of information, it was necessary to calculate this parameter.

On the other hand, we can discard the "take off and climb" as well as the "descent and land" because even in those moments the UAV is using four motors. This short period of time makes these two profiles irrelevant with respect to the total power consumption of the UAV for an entire mission.

F. POWER GENERATED FROM THE SOLAR CELLS

Next, we turned our attention to the solar array. The first step was to determine the amount of power available from the use of a solar array. The equation below gives the power P_{solar} that can be generated from a solar array [55].

$$\boldsymbol{P_{solar} = I\, cos(i)\, S_c\, \eta_{total}}$$

where I is the solar irradiance in a specific location of the Earth, S_c is the area of the solar cell array that basically equals the wingspan area, i is the angle between the line of sight to the sun and the solar array normal, and η_{total} is the efficiency of the solar cells that is already known [55]. For the solar irradiance I, we used a nominal value of 0.1 W/cm^2 [55].

1. Wing Area S_c of the Nimbus Pro VTOL

We needed a value for the wing area as this was the surface onto which the solar array would be attached. To find this value, we printed an image of the Nimbus Pro VTOL onto graph paper. Only the overall dimensions of the aircraft were available, but this was all that was needed to find the additional values required. Using the image, we determined

that each square was equal to approximately 2.41 cm/square. With this scale factor, the additional dimension of the wing—the wing chord length—was found to be approximately 32 cm. Figure 54 shows the wing's cross section, as well as its measurements. The wingspan of the original Nimbus Pro VTOL wing is ~190 cm and the chord is ~32 cm; multiplying both values we could get the wingspan area of the Nimbus Pro VTOL.

$$S_c = 190 \text{ cm} \times 32 \text{ cm} = 6080 \text{ cm}^2$$

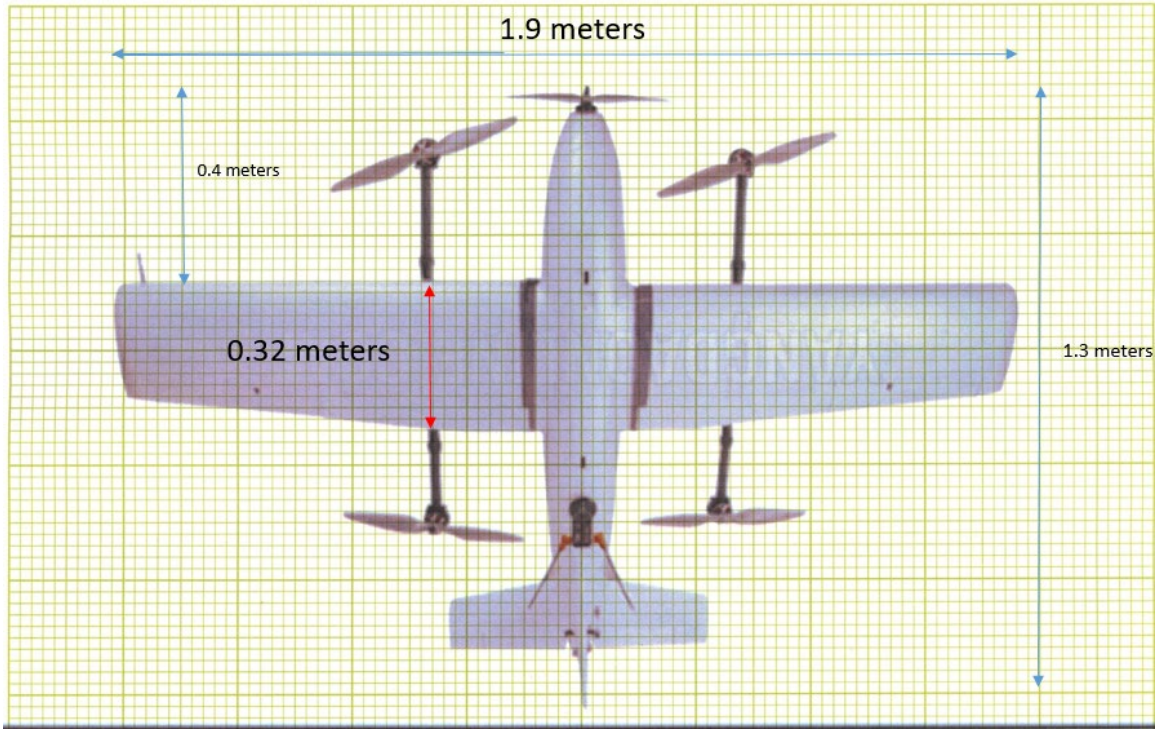

Figure 54. Nimbus Pro VTOL dimensions. Source: [56].

2. Total Efficiency η_{total} CIGS Solar Cell

The solar efficiency of the CIGS solar cell in this specific case is 15% [57]. It is important to mention that CIGS solar cells already exist with a 17% efficiency, however [57].

3. Determining the Angle of Incidence

The term $\cos(i)$ uses the angle between the line of sight to the sun and the solar array normal [55]. The term accounts for the geometry between the sun and the solar panel array and affects the maximum power we could expect to produce. This relationship is depicted in Figure 55 with the angle of incidence *i* represented with the symbol θ.

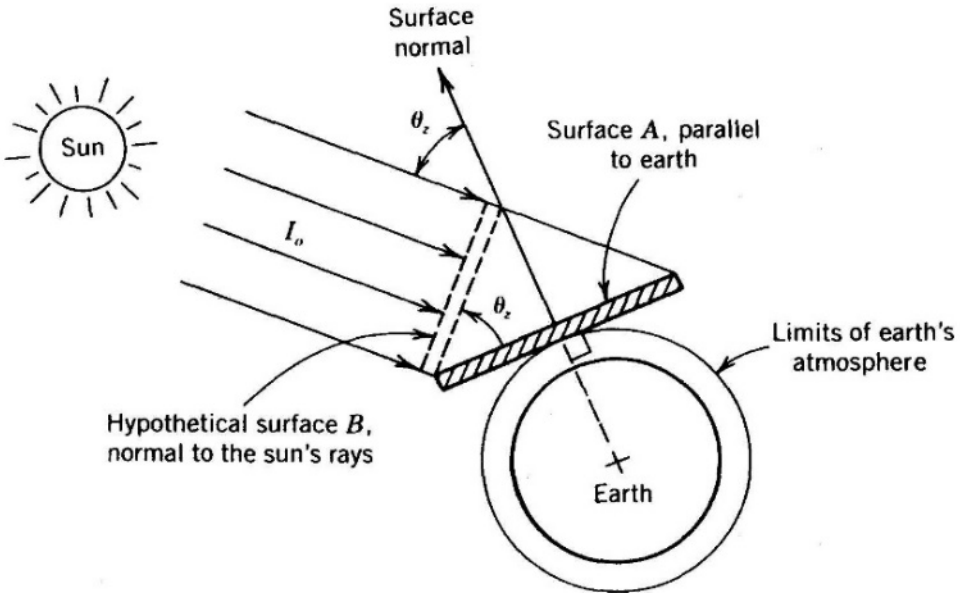

Figure 55. Solar irradiance on a parallel to the ground surface

To understand the influence of the $\cos(i)$ term, we considered first the angles of the sun. These angles, namely the azimuth and elevation, vary around the world and throughout the year. For our analysis, we selected the north of Peru. In [54], we find the procedure to compute the sun angles, but instead we opted to use information available online, such as from [58]. Resources such as these are available online for commercial and residential installers who use the sun angles to decide the best orientation to install a solar panel at a given location. In Figure 56 and Figure 57, the sun angles are shown for the summer and winter solstice in the north of Peru. These figures show how the azimuth and elevation vary throughout a 24-hour period. From the plots, we found that during the summer solstice the azimuth and elevation sun angles are 190.2 degrees and 78.42 degrees,

respectively, during solar noon time, which is the time at which the maximum elevation angle occurs. For the winter solstice, we found that the azimuth angle is -2.05 degrees and the elevation angle is 54.5 degrees during solar noon. As we might expect, the sun elevation is more than 20 degrees higher in the summer than in the winter. Although the summer solstice has the sun at its highest elevation of the year and winter solstice has the lowest sun angles, these figures are used to develop an understanding of the influence of the $\cos(i)$ term and its impact on the best- and worst-case scenarios for the generation of power from the solar array.

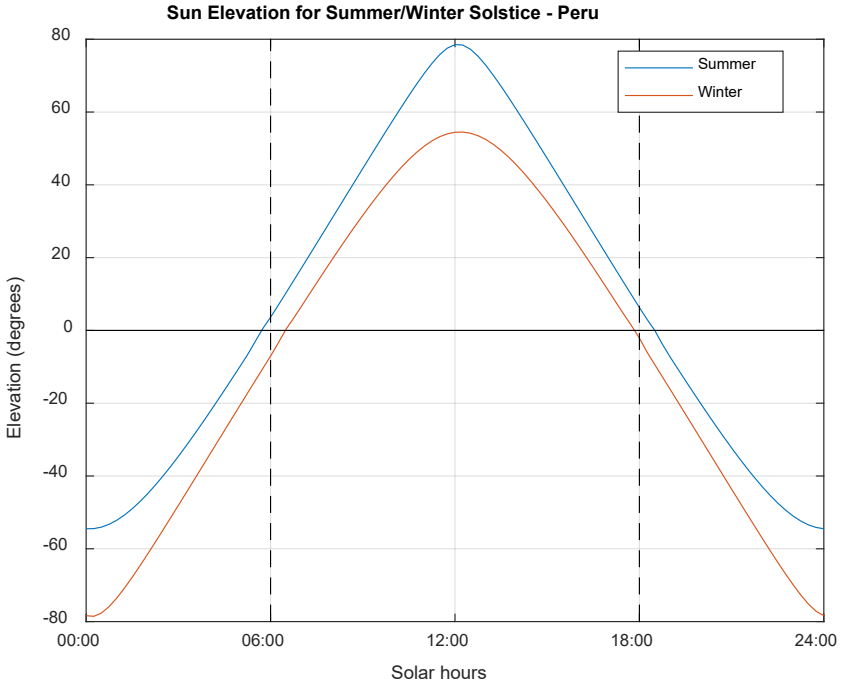

Figure 56. Sun elevation for summer/winter solstice – Peru

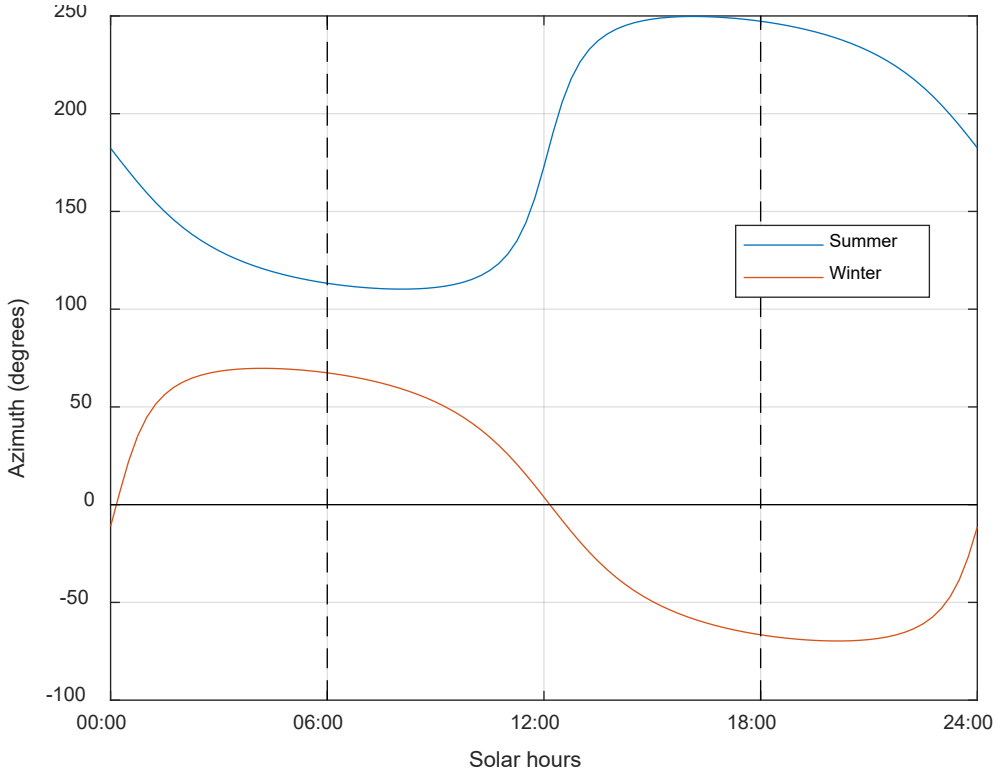

Figure 57. Sun azimuth for summer/winter solstice – Peru

Using the sun angles for the summer and winter solstice at solar noon, we computed the $\cos(i)$ term as it varies for a typical maneuver of a 10-degree banked turn of the aircraft. As we can see in Figure 58, the variation in $\cos(i)$ is expected depending on the season. In the figure, we can appreciate that the maximum value (best case scenario) is 1.0, which means that the wings or solar cells normally are in the same line of sight to the sun making an angle of 0 degrees. The lowest value is 0.7 in the winter, however, which would reduce the power available from the solar panel to 70% of its maximum.

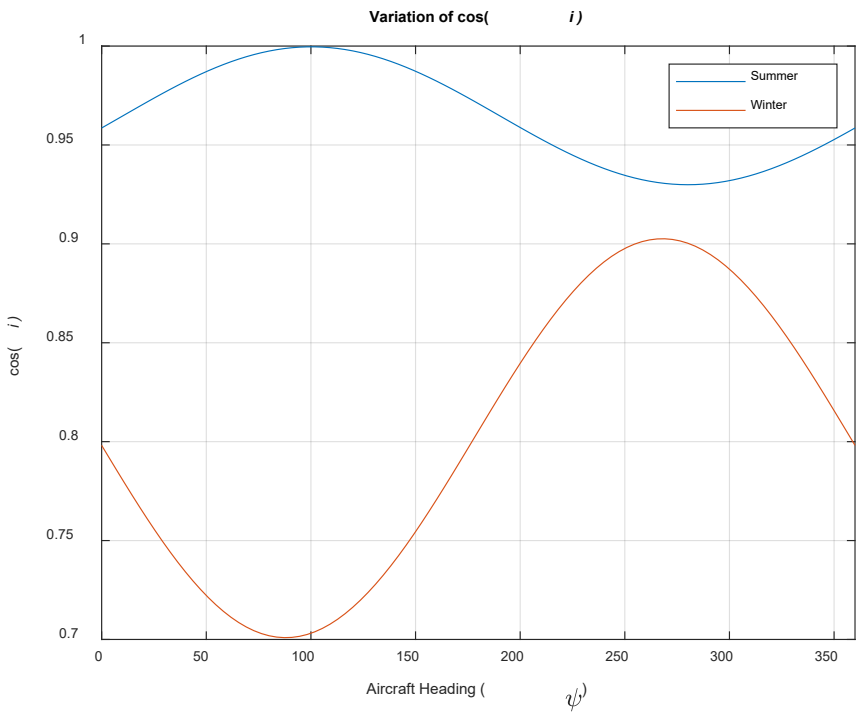

Figure 58. Simulation of the aircraft making a 360-degree turn

4. Obtaining the Irradiance

The amount of irradiance from the sun is largely steady and spreads at a predictable rate. At the typical distance between the Earth and the sun, this solar constant I is acknowledged to have a power density of 1367 W/m^2 [55].

The majority of research simulating normal circumstances at latitudes in North America utilizes an air mass of 1.5 (AM1.5), which amounts to a power density of 1000 W/m^2 [55]. We determined that for this particular case, since the experiment was theoretical, we had to consider an average irradiance of 0.1 W/cm^2 (1000 W/m^2) [55].

5. Calculations

Having obtained the values for each variable of the equation, we proceeded to compute the power generated by the solar cells in the following relation, taking into consideration the best scenario.

$$P_{solar} = I_{cos}(i) S_c \eta_{total}$$

$$P_{solar} = 0.1 W/cm^2 \times \cos(0) \times 6080 cm^2 \times 0.15$$

$$P_{solar} = 91.2 Watts$$

G. PERFORMANCE ANALYSIS

The specifications from the manufacturing company stated the maximum flying time of the Nimbus Pro VTOL is 100 minutes. Based on our estimates, the power consumption would be ~180 watts. The power generated from the solar cells, however, was approximately 91.2 watts utilizing flexible CIGS solar cells, which have an efficiency of 15%. In the following table and equation, we will show a comparison of the UAV with and without solar cells, as well as the additional amount of flying time resulting from the use of the solar array. We determined after the calculations that the Nimbus Pro VTOL with solar cells could fly ~199 minutes—99 minutes more than what the manufacturer offers.

Profile	Time (hr)	Throttle (%)	Power consumed by the payloads (W)	Amount of motors used	Total power from the motors (W)	Total Energy consumed (Wh)
Starting Capacity of battery						520
Take off and climb	0.022	85%	65	115 Watts x 4	460	-11.55
Take off and climb with Solar array	0.022				91.2	2
Orbit/Maneuvering	t	56.30%	65	115 Watts	115	-180
Orbit/Maneuvering with Solar array	t				91.2	91.2
Descent and Land	0.038	0.00%	65	115 Watts x 4	460	-19.95
Descent and Land with Solar array	0.038				91.2	3.47
Total Power left						199.42

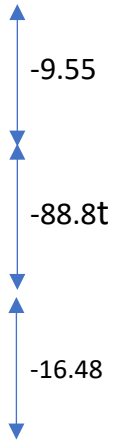

Table 8. Performance analysis of the UAV with and without solar cells

$$520 - 9.55 - 88.8t - 16.48 = 199.42$$

$$t = 3.32hr = 199\,\text{min}$$

THIS PAGE INTENTIONALLY LEFT BLANK

VIII. CONCLUSION

In this research, we started by identifying a problem with the use of SUAVs in the armed forces of the U.S. We noticed a prominent issue with the useful endurance of these vehicles and that the available flying time was not long enough for the completion of important missions. We started looking for a new and better option, taking into account the devices and payload that this new vehicle could support. After a long research period and comparing different models, we decided to work with the Nimbus Pro VTOL UAV because it was the latest generation of flying vehicle on the market with the highest level of technology.

We then looked for a way to improve the flying time of this particular UAV beyond the 100 minutes indicated by the manufacturer, which is not enough time for a long surveillance mission. This research considered the use of flexible solar cells to obtain power from the sun to compensate the loss of power from the batteries, which were the common and widely-used lithium-ion batteries. We considered that the best option was the CIGS solar cells because of its flexibility to fit on the curvature of the aircraft wing, high efficiency of 15% and 17%, and low cost compared with other similar solar cell technology. It is important to know that there are some others that have more efficiency on the market, but they are extremely expensive to cover a large wing area of a UAV.

Our initial plan was to purchase a Nimbus Pro VTOL aircraft for real experimental work and to quantify the improvement to the endurance of this UAV. Due to budgetary restrictions and the limited schedule, however, we were unable to acquire one of these flying vehicles.

In spite of this minor inconvenience, we began the analysis by making a hypothetical flight obtaining an approximate estimate of power consumption, taking into account important details of the vehicle such as the battery capacity, number of motors, servos, time of flight, and throttle settings that were presented on a regular flight profile without solar cells. On the other hand, it was really important to know how much power we would generate from the solar cells, but to this kind of measure we had to take into

consideration important variables such the solar irradiance, angle of inclination of the wing with respect to the sun, wingspan area of the UAV, and efficiency of the solar cell. After those calculations, we determined a second flight profile where we established that instead of flying 100 minutes without solar cells, we could achieve a longer flight time of 199 minutes in the best conditions, which almost doubles the flight time of this particular SUAV. This is relevant for missions of surveillance patrol and monitoring of the territory.

LIST OF REFERENCES

[1] J. Guilmartin, "Unmanned aerial vehicle," Encyclopedia Britannica, blog, 2020. https://www.britannica.com/technology/unmanned-aerial-vehicle

[2] L. Mansfield, "Copper indium gallium diselenide solar cells," Photovoltaic Research, blog. https://www.nrel.gov/pv/copper-indium-gallium-diselenide-solar-cells.html (accessed Oct. 24, 2021).

[3] AeroVironment, Inc, "Puma™ 3 AE," AV AeroVironment, blog, 2021. https://www.avinc.com/uas/puma-ae

[4] K. Vyas, "A brief history of drones: The remote controlled unmanned aerial vehicles (UAVs)," Interesting Engineering, blog, 2020. https://interestingengineering.com/a-brief-history-of-drones-the-remote-controlled-unmanned-aerial-vehicles-uavs

[5] I. Ridwan, "The effect of use of solar panels on micro scale fixed-wing UAV type as a power recharging system," AIP Conference Proceedings, blog, 2019. https://aip.scitation.org/doi/abs/10.1063/1.5135553

[6] C. Gromadski, "Extending the endurance of small unmanned aerial vehicles using advanced flexible solar cells," M.S. thesis, Dept. of ECE, Naval Postgraduate School, Monterey, CA, USA, 2012.

[7] W. Hurd, "Application of copper indium gallium diselenide photovoltaic cells to extend the endurance and capabilities of unmanned aerial vehicles," M.S thesis, Dept. of ECE. Naval Postgraduate School, 2009.

[8] J. Cova, "Application of copper indium gallium diselenide photovoltaic cells to extend the endurance and capabilities of the Raven RQ-11B unmanned aerial vehicle," M.S thesis, Dept. of ECE. Naval Postgraduate School, 2010.

[9] C. Keen Chin, "Extending the endurance, missions and capabilities of most UAVS using advanced flexible/ridged solar cells and new high power density batteries technology," M.S. thesis, Dept. of ECE. Naval Postgraduate School, 2011.

[10] AeroVironment, Inc, "Raven datasheet," AV AeroVironment, blog, 2017. https://www.avinc.com/images/uploads/product_docs/Raven_Datasheet_2017_Web_v1.pdf

[11] Wingtra, "Fixed-wing drones: the evolution of the technology," Wingtra, blog, 2021. https://wingtra.com/fixed-wing-drones-the-evolution/

[12] AeroVironment, Inc, "Puma™ 3 AE," AV AeroVironment, blog, 2021. https://www.avinc.com/uas/puma-ae

[13] Yochim, "The vulnerabilities of unmanned aircraft system common data links to electronic attack," M.S. thesis, General Studies, B.S., Weber State University, Ogden, Utah, 1998.

[14] Preneu, "MILVUS from aerial survey to security monitoring," Preneu, blog. https://www.preneu.com/milvus-en/ (accessed Nov. 02, 2021).

[15] Drone File, "Foxtech: Providing cost-effective solutions for enterprise drone mapping missions," Drone Life, blog, 2018. https://dronelife.com/2018/07/20/foxtech-providing-cost-effective-solutions-for-enterprise-drone-mapping-missions/

[16] Drone Engr, "Nimbus VTOL V2 PNP aircraft," Drone Engr, blog, 2021. https://www.droneassemble.com/product/nimbus-vtol-v2-pnp-aircraft-for-mapping-and-survey/

[17] C. Honsberg, "CIGS solar cells overview," pveducation, blog, 2016. https://www.pveducation.org/pvcdrom/cigs-solar-cells-overview

[18] B. Chapman, "How does a lithium-ion battery work?" Let's Talk Science, blog, 2019. https://letstalkscience.ca/educational-resources/stem-in-context/how-does-a-lithium-ion-battery-work

[19] M. Mirzaeian, "Lithium ion battery," Science Direct, blog, 2012. https://www.sciencedirect.com/topics/chemistry/lithium-ion-battery

[20] Office of Energy Efficiency & Renewable Energy, "How does a lithium-ion battery work?" Energy, blog, 2017. https://www.energy.gov/eere/articles/how-does-lithium-ion-battery-work

[21] Fujitsu Siemens, "How to rebuild a Li-ion battery pack," Electronics Lab, blog, 2019. https://www.electronics-lab.com/

[22] Electronics Notes, "Lithium-ion battery advantages & disadvantages," Electronics Notes, blog. https://www.electronics-notes.com/articles/electronic_components/battery-technology/li-ion-lithium-ion-advantages-disadvantages.php (accessed Oct. 20, 2021).

[23] University of Washington, "Lithium-ion battery," Clean Energy Institute, blog, 2020. https://www.cei.washington.edu/education/science-of-solar/battery-technology/

[24] R. Fonash, "Solar cell," Encyclopedia Britannica, blog, 2020. https://www.britannica.com/technology/solar-cell

[25] Jestin, “Photovoltaic solar energy,” Comprehensive Renewable Energy, blog, 2012. https://www.sciencedirect.com/topics/engineering/solar-spectrum

[26] The Editors of Encyclopaedia Britannica, “Electromagnetic spectrum,” Encyclopedia Britannica, blog, 2019. https://www.britannica.com/science/electromagnetic-spectrum

[27] F. Dunnivant, “The Interaction of electromagnetic radiation with sample molecules,” People Whitman, blog, 2008. http://people.whitman.edu/~dunnivfm/FAASICPMS_Ebook/CH1/1_2.html

[28] Office of Energy Efficiency & Renewable Energy, “Solar radiation basics,” Energy, blog, 2017. https://www.energy.gov/eere/solar/solar-radiation-basics

[29] A. Harvey, “The modification of homer software application to provide the United States Marine Corps with an energy planning tool,” M.S. thesis, Dept. of ECE. Naval Postgraduate School, Monterey, CA, 2012.

[30] C. Honsberg, “Average solar radiation,” pveducation, blog. https://www.pveducation.org/pvcdrom/properties-of-sunlight/average-solar-radiation (accessed Oct. 20, 2021).

[31] B. Afework, “Photovoltaic cell,” Energy Education, blog, 2021. https://energyeducation.ca/encyclopedia/Photovoltaic_cell

[32] Ossila, “Solar cells: A guide to theory and measurement,” Ossila, blog, 2021. https://www.ossila.com/pages/solar-cells-theory

[33] M. Powalla, “Advances in cost-efficient thin-film photovoltaics based on Cu(In,Ga)Se2,” Science Direct, blog, 2017. https://www.sciencedirect.com/science/article/pii/S2095809917306033

[34] H. Sainthiya, “Basic diagram of photovoltaic solar cell,” Research Gate, blog, 2017. https://www.researchgate.net/figure/Basic-diagram-of-Phtovoltaic-solar-cell_fig1_323354575

[35] T. Segal, “Semiconductor,” Investopedia, blog, 2021. https://www.investopedia.com/terms/s/semiconductor.asp

[36] R. Nave, “Bands for doped semiconductors,” Hyperphysics, blog. http://hyperphysics.phy-astr.gsu.edu/hbase/Solids/dsem.html (accessed Nov. 02, 2021).

[37] A. Augustyn, “The p-n junction,” Encyclopedia Britannica, blog. https://www.britannica.com/science/semiconductor/The-p-n-junction (accessed Nov. 05, 2021).

[38] D. Jordan, “Photovoltaic degradation rates—An analytical review,” *Natl. Lab. U.S.,* vol. 62, no. 2, p. 32, Jun. 2012.

[39] “Solar cell efficiency,” *Wikipedia*. Accessed: Oct. 15, 2021. [Online]. Available: https://en.wikipedia.org/wiki/Solar_cell_efficiency

[40] Niclas, “CIGS solar cells,” Sino Voltaics, blog. https://sinovoltaics.com/learning-center/solar-cells/cigs-solar-cells/ (accessed Dec. 02, 2021).

[41] L. Mansfield, “Copper indium gallium diselenide solar cells,” Photovoltaic Research, blog. https://www.nrel.gov/pv/copper-indium-gallium-diselenide-solar-cells.html (accessed Oct. 24, 2021).

[42] Maker.io, “Introduction to DC-DC converters,” Digi-Key, blog, 2016. https://www.digikey.com/en/maker/blogs/introduction-to-dc-dc-converters

[43] Components101, “Boost converter basics working design,” Components, blog. https://components101.com/articles/buck-converter-basics-working-design-and-operation (accessed Nov. 11, 2021).

[44] “Buck converter,” *Wikipedia*. Accessed: Nov. 15, 2021. [Online]. Available: https://en.wikipedia.org/wiki/Buck_converter

[45] G. Harper, “CIGS solar cell,” Encyclopedia Britannica, blog, 2016. https://www.britannica.com/technology/CIGS-solar-cell

[46] Office of Energy Efficiency & Renewable Energy, “Copper indium gallium diselenide,” Energy, blog. https://www.energy.gov/eere/solar/copper-indium-gallium-diselenide (accessed Nov. 05, 2021).

[47] Mr. Solar, “What is maximum power point tracking and how does it work?” Mr. Solar, blog, 2022. https://www.mrsolar.com/what-is-maximum-power-point-tracking-and-how-does-it-work/

[48] PSCAD, “Maximum power point tracker (for photovoltaic source),” PSCAD, blog. https://www.pscad.com/webhelp/Master_Library_Models/Sources /Maximum_Power_Point_Tracker.htm (accessed Dec. 05, 2021).

[49] Sudha, “Solar energy for extension of endurance for unmanned air vehicle,” IJERT, blog, 2018. https://www.ijert.org/solar-energyfor-extensionof-endurance-for-unmanned-air-vehicle

[50] N. Camacho, “Improving operational effectiveness of tactical long endurance unmanned aerial systems (Taleuas) by utilizing solar power,” M.S. thesis, Dept. of ECE. Naval Postgraduate School, 2014.

[51] Z. Yang, “State of art on energy management strategy for hybrid-powered unmanned aerial vehicle,” Science Direct, blog, 2019. https://www.sciencedirect.com/science/article/pii/S1000936119301268

[52] Millswood, “Battery balancers,” Millswood Engineering, blog, 2021. https://millswoodeng.com.au/battery_balancers.html

[53] HobbyKing, “Turnigy Aerodrive sk3 2822-1740kv brushless outrunner motor” HobbyKing Online, blog. https://www.hobbyking.com/en_us/ (accessed Feb. 17, 2022)

[54] D. J. Edwards, A. D. Kahn, M. Kelly, S. Heinzen, D. A. Scheiman, P. P. Jenkins, R. Walters, and R. Hoheisel, “Maximizing net power in circular turns for solar and autonomous soaring aircraft,” *Journal of Aircraft,* vol. 53, no. 5, pp. 1237–1247, 2016.

[55] C. Perez, “Increasing performance of the RQ-20 Puma with photovoltaic cells,” M.S. thesis, Dept. of ECE. Naval Postgraduate School, 2018.

[56] Yangda, “Yangda Nimbus Pro VTOL fixed-wing drone for mapping and surveillance,” Yangda Online, blog. https://www.yangdaonline.com/yangda-nimbus-pro-vtol-fixed-wing-drone-for-mapping-and-surveillance/ (accessed Nov. 16, 2021).

[57] D. Bremaud, D. Rudmann, G. Bilger, H. Zogg and A.N Tiwari, “Towards the development of flexible CIGS solar cells on polymer films with efficiency exceeding 15%,” Physics Group, vol. 3, no. 11, pp. 1–4, 2005.

[58] Keisan, “Keisan online calculator,” Keisan Casio, blog. https://keisan.casio.com/exec/system/1224682277 (accessed Jan. 10, 2022)

THIS PAGE INTENTIONALLY LEFT BLANK

INITIAL DISTRIBUTION LIST

1. Defense Technical Information Center
   Ft. Belvoir, Virginia

2. Dudley Knox Library
   Naval Postgraduate School
   Monterey, California